Cloning and expression of Cyt2Aa1 toxin and characterization of its mode of action

by

Mohamed S. Abdel Rahman

A thesis
presented to the University of Waterloo
in fulfillment of the
thesis requirement for the degree of
Master of Science
in
Biology

Waterloo, Ontario, Canada, 2010

Author's Declaration

I hereby declare that I am the sole author of this thesis. This is a true copy of the thesis, including any required final revisions, as accepted by my examiners.

I understand that my thesis may be made electronically available to the public.

Abstract

The discovery of the pore-forming toxins produced by *Bacillus thuringiensis*, which are toxic to insects but not to mammalians, has provided a new successful means to control harmful plant-feeding insects biologically. The toxins are also used on insects that don't feed on plants, for example on *Anopheles.* The *Bacillus thuringiensis* toxins fall into two structural families, named *cry* and *cyt*. All of these toxins act by damaging the cell membranes in the mid gut of the insect. In this study, a reliable system for expression and purification of the recombinant Cyt2Aa1 toxin has been developed. The recombinant Cyt2Aa1 toxin has been produced, characterized, followed by the construction of the cysteine mutantsV186C and L189C by site directed mutagenesis. The new expression system yields 0.4g of protein per litre of culture. The activated Cyt2Aa1 toxin is active in the hemolysis assay. Of note, the hemolytic activity of the V186C mutant exceeds that of wild type Cyt2Aa1 toxin and of the L189C mutant. Calcein release assay experiments have been done to examine the activity of the toxin with different artificial liposomes. It was found that Cyt2Aa1 toxin is very active with DMPC, DMPC+DMPG unilamellar liposomes. Surprisingly, however, Cyt2Aa1 toxin showed no activity with liposomes containing cholesterol. With both erythrocytes and sensitive liposomes, the toxin shows a "pro-zone effect", that is the activity decreases at very high concentrations. The findings are discussed in the context of the toxin's putative mode of action.

Acknowledgements

First of all, I would like to express my special thanks to Dr. Michael Palmer for his supervision, advice, and guidance. He supported me with unwavering encouragement in various ways. I owe so much gratitude and appreciation to him more than he knows.

I would like to extend my thanks to my advisory committee members, Dr. Guy Guillemette and Dr. Trevor Charles for their useful suggestions and comments.

I would like to thank my lab members Lisa Pokrajac, Jawad Muraih , Oscar Zhang and Eric Brefo-Mensah for their support.

Finally, I would like to express my gratitude to my wonderful wife Neveen, for her patience and support.

Dedication

To my beloved wife and my little two angels

To my father and brothers

To the soul of my mother

To everyone supported me

Table of Contents

List of Figures

List of Tables

List of Abbreviations

Bt: *Bacillus thuringiensis*

Cry: Crystal insecticidal proteins of *Bt*

Cyt: Cytolytic insecticidal proteins of *Bt*

DMPC: 1,2-dimyristoyl-*sn*-glycerol-3-phosphocholine

DMPG: 1,2-Dimyristoyl-*sn*-glycero-3-phosphoglycerol

 DNTP: deoxynucleoside triphosphate

FRET: Fluorescence resonance energy transfer

HEPES**:** N-(2-Hydroxyethyl)-piperazine-N´-(2-ethanesulfonic acid)

IPTG: Isopropyl-β-D-thiogalactopyranoside

LB: Luria Bertani broth

OD: Optical density

PC: Phosphatidylcholine

PCR: Polymerase chain reaction

PDB: Protein Data Bank

PFT: Pore-forming Toxins

PMSF: Phenylmethylsulfonyl fluoride

rpm: Rotations per minute

RBCs: Red Blood Cells

SDS: Sodium dodecylsulfate

SDS-PAGE: SDS-polyacrylamide gel electrophoresis

UV: Ultraviolet

1 Introduction

There is a high demand to control the population of harmful insects all over the world. One reason for this is the transmission of dangerous diseases like malaria or yellow fever by well-known insects. The control of harmful insect species in agriculture has long been of concern because of the dire need for increasing crop yields **[i]**. Many chemical insecticides have been discovered and used for controlling harmful insects; examples are DDT, carbamates and organophosphates. However, many of those chemical insecticides may compromise human health, as they may cause cancer, liver damage, impotence and birth defects **[ii]**.

The discovery of the pore-forming toxins produced by *Bacillus thuringiensis*, which are toxic to insects but not to mammalians, has provided a new successful means to control of harmful insects biologically **[iii]**. The *Bacillus thuringiensis* toxins fall into two structural families, named *cry* and *cyt*. All these toxins act by forming oligomeric pores in the cell membranes of the mid gut of the insect **[iv]**. This study focuses on Cyt2Aa1, a member of the *cyt* family. The goal of this study was to develop a reliable system for cloning, expression and purification of the recombinant Cyt2Aa1 toxin and to elucidate its mechanism of action. To achieve this, recombinant Cyt2Aa1 toxin has been produced, characterized, followed by the construction of V186C and L189C cysteine mutants obtained by site directed mutagenesis. Fluorescent marker release assays have been done with liposomes of different lipid composition to examine the activity of the toxin.

1.1   Pore-forming toxins

Pore-forming proteins and peptides are among nature's most potent biological weapons. They are typically secreted as water-soluble, monomeric proteins, but after they reach their target membrane, they are transformed into membrane proteins that enclose a central pore, which permeabilizes the membrane. This transformation involves extensive conformational changes [v]. The pore-forming toxins (PFTs for short) form pores in the lipid bilayers of cell membranes, which causes osmotic imbalance and subsequently leads to cell swelling, lysis and death [vi]. Pore-formation is a major and widespread mechanism for toxin-mediated cell attack in bacteria, plants, fungi, insects and animals [v]. Pore-forming toxins may also translocate toxic enzymes across the membrane, as is the case with diphtheria, cholera and pertussis toxins.

1.1.1   Classification of pore forming toxins

PFTs can be classified according to some specific characteristic that is required for activity or according to the organisms that produce them [vii]. A particularly useful classification is based on certain structural features [v]. The α-PFTs are mostly α-helical in structure. These toxins have pore-forming domains consisting of a three-layer structure with up to ten α-helices sandwiching a hydrophobic helical hairpin in the middle of the structure (see **Figure 1**). These toxins tend to form pores by using helices, and the central hairpin is thought to drive the initial step of the insertion process.

A

B

C

D
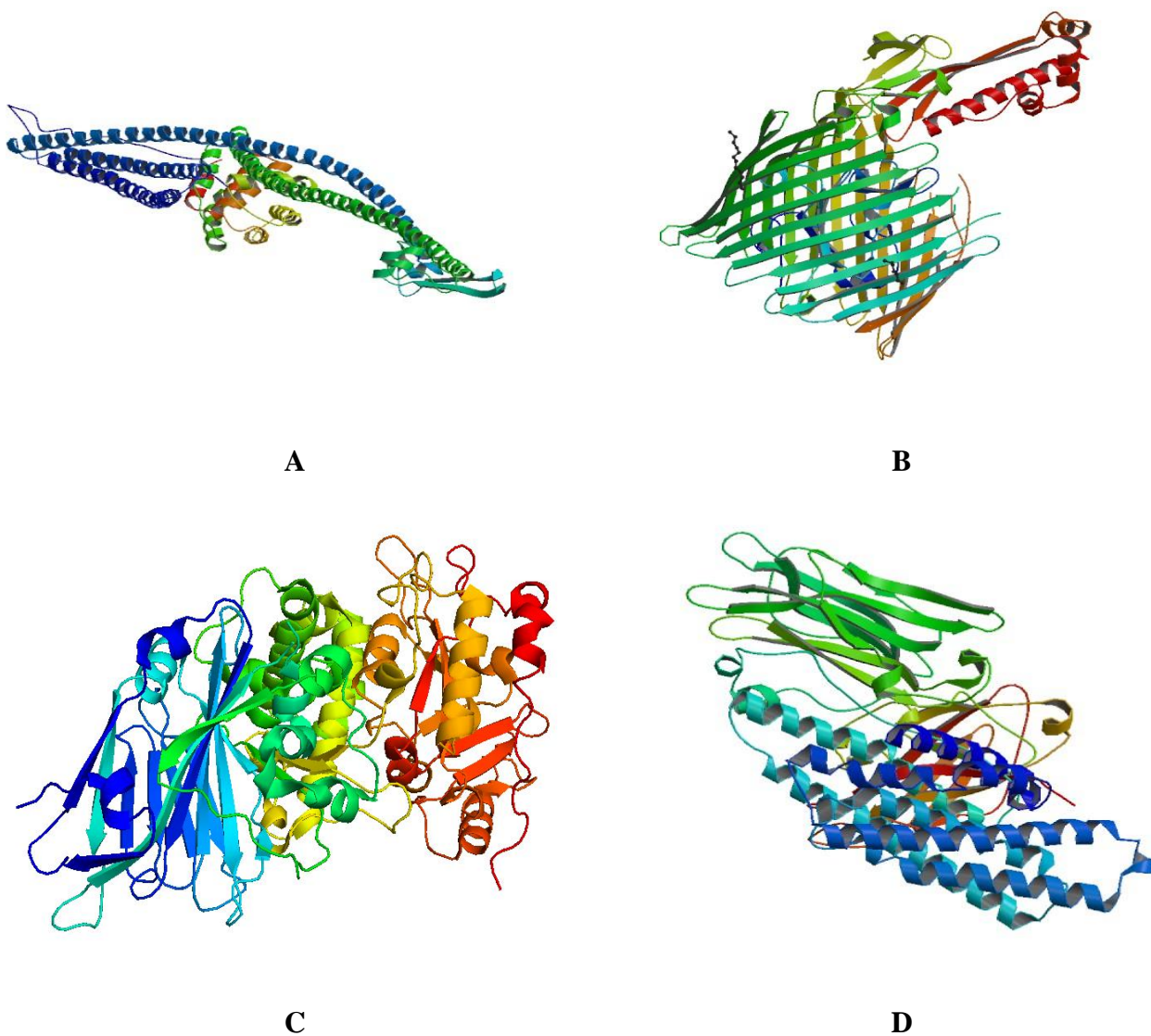
Figure 1: Ribbon representation of α-PFT structures. A: Colicin Ia (PDB entry 1CII) **[viii]** ; B: Colicin I receptor complex with receptor binding domain of Colicin Ia (PDB entry 2HDI)**[ix]** ; C: *Pseudomonas aeruginosa* exotoxin A (PDB entry 1IKQ) **[x]** ; D: Cry3Bb1 *Bacillus thuringiensis* insecticidal δ-endotoxin (PDB entry 1JI6) **[xi]**. These structures were rendered from PDB records using Pymol **[xxxiv].**
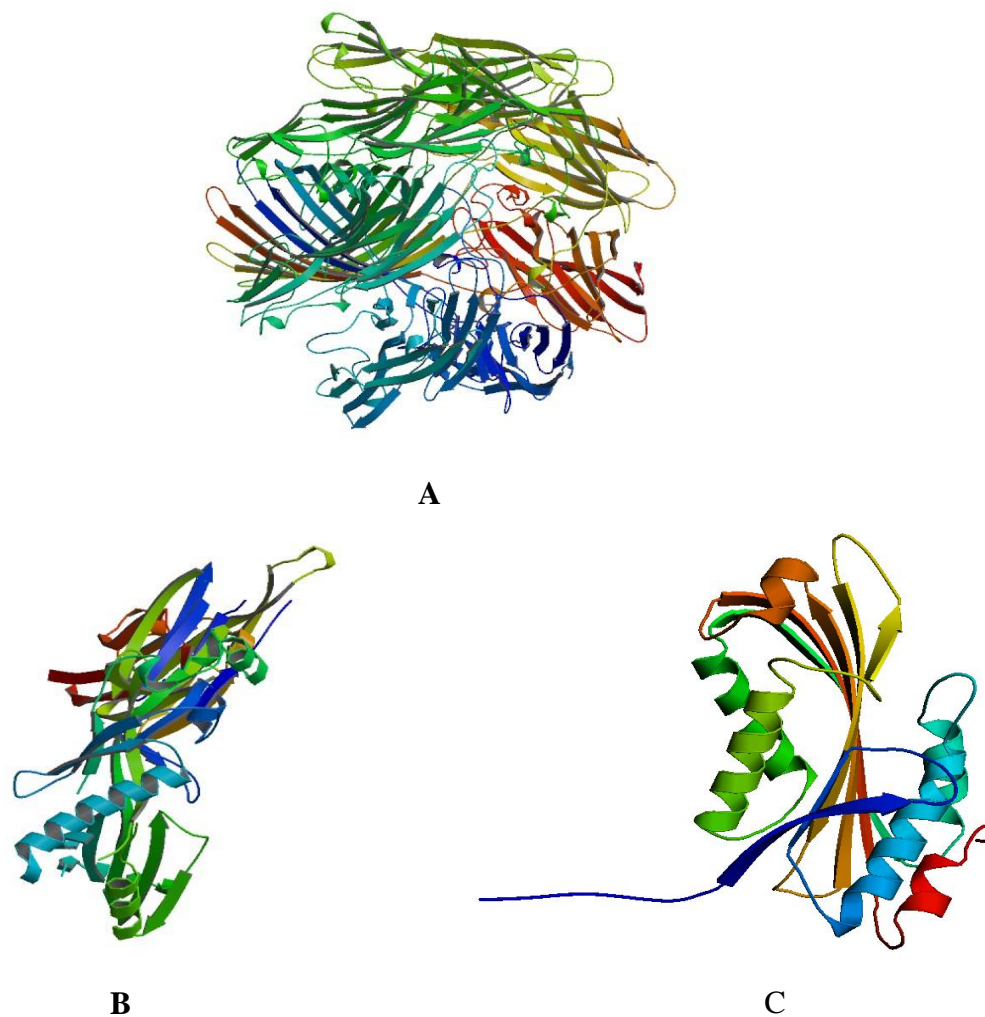
Figure 2 : Ribbon representation of β-PFT structures. A: The heptameric pore formed by *Staphylococcus aureus* α-hemolysin (PDB entry 7AHL) **[xii]** B: *Clostridium perfringens* perfringolysin O (PDB entry 2BK1) **[xiii]**; C: *Bacillus thuringiensis* Cyt2Aa1 δ-endotoxin monomer (PDB entry 1CBY) **[xiv]**. These structures were rendered from PDB records using Pymol **[xxxiv].**

4

Another major class of pore-forming toxins, termed the β-PFTs, insert into membranes to form a β-barrel (see **Figure 2**.A). These toxins tend to be rich in β-sheet.

1.1.2 General mechanism of pore formation

The basic steps involved in the generation of pores by PFTs have been understood for a long time and are summarized in **Figure 3**. Briefly, after the protein toxin is secreted from the bacterium, the toxin molecules bind to their target cells via specific surface receptors, which can be specific proteins or lipids. Some toxins can attach to cells without the need for any kind of receptor. The current doctrine declares that the receptor concentrates the toxin on the cell surface and so facilitates the formation of oligomers on the cell surface **[v,vii]**. The oligomerized toxin then starts to insert partially or completely into the lipid bilayer of the cell membrane. The inserted part may adopt a β-barrel or α-helical structure. The pores may be of different sizes **[v]**.

Bacterial cell

Toxin

Toxin is secreted then binds to receptors on the cell surface (in most cases)

Host cell

Oligomerization of molecules

Insertion into the cell membrane
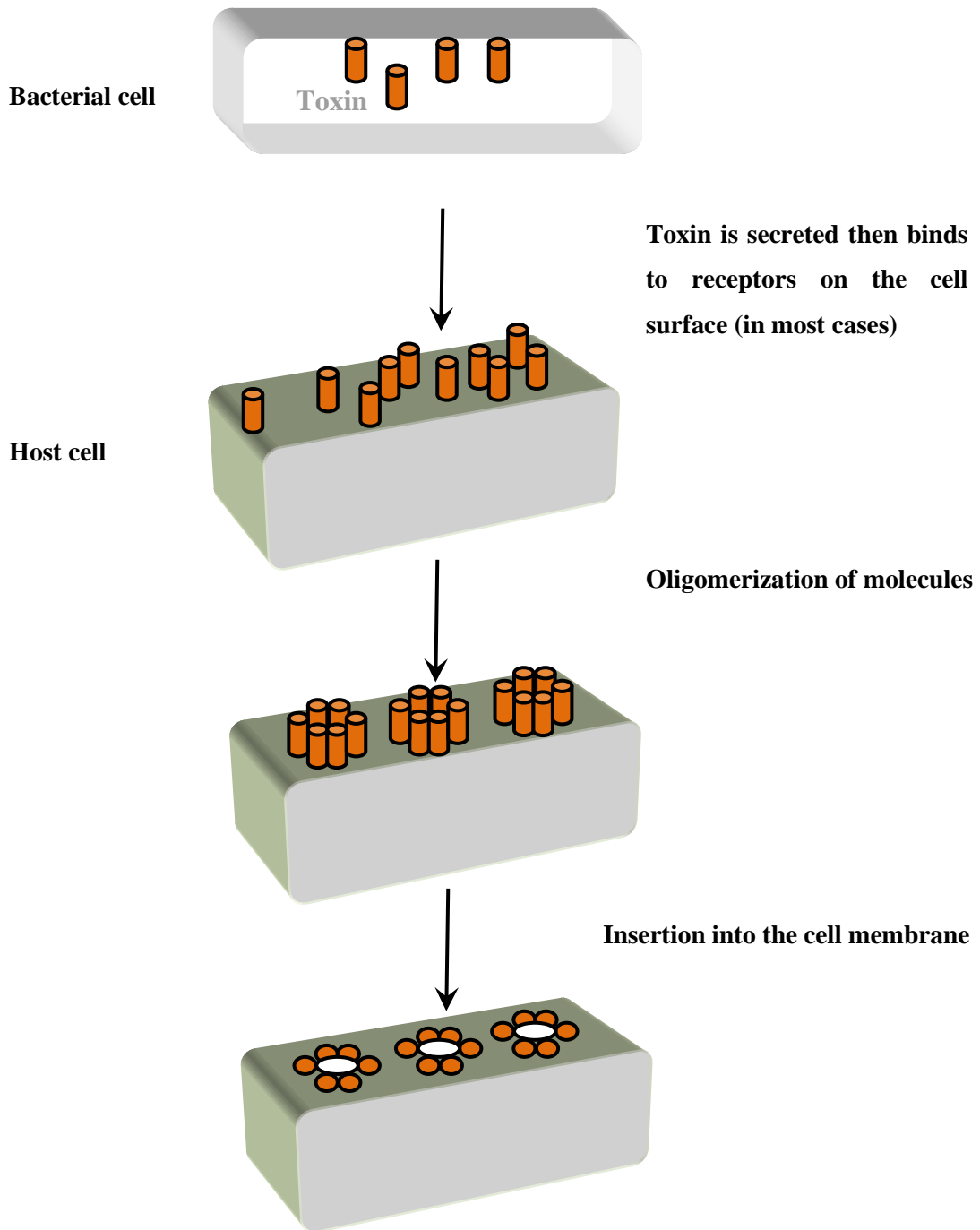
Figure 3 : The general steps involved in membrane pore formation generated by PFTs **[v]**.

1.2   Bacillus thuringiensis and its toxins

In 1901, the soil bacterium *Bacillus thuringiensis* (*Bt* for short), was discovered in Japan by Ishawata and in 1911 in Germany by Berliner. *Bacillus thuringiensis* is an aerobic, gram-positive, endo-spore-forming bacterium. The species comprises numerous strains, each of which produces its own unique combination of insecticidal protein toxins during sporulation **[iii]**. Bacillus thuringiensis (*Bt*) toxins are also known as δ-endotoxins. Variations in insecticidal specificity of those toxins have been observed between different *Bt* strains. However, the entire set of *Bt* δ-endotoxins affects many species from the orders of Diptera, Lepidoptera, and Coleoptera **[xv]**. Commercial *Bt* products are powders containing a mixture of crystallized toxins and dried spores, which are applied to crops or leaves where the insect larvae feed. Nowadays, the genes of some *Bt* δ-endotoxin have been introduced into crop plants like cotton and maize, which renders these plants toxic for insects feeding on them. Humans and other mammals are unaffected because the Bt toxins are contained in the cells in insoluble form and undergo proteolytic activation in the insect gut, which releases the active monomer **[xvi]**.

1.2.1   General structure and classification of Bt δ-endotoxins

There are two major classes for *Bt* toxins based on the amino acid sequence of the toxins, referred to as the *cry* (Crystal) family and the *cyt* (Cytolytic) family respectively **[xvii]**.

1.2.1.1 Cry toxins

For the *cry* toxins, more than two hundred known members with not less than 50 subgroups have been distinguished in the *cry* family based on their amino acid sequence (see **Table 1**). All of them share the same pattern in structure but differ in their degree of binding specificity and toxicity [**xvii**]. Up to now, the crystal structures of six different *cry* toxins (Cry1Aa, Cry2Aa, Cry3Aa, Cry3Bb, Cry4Aa and Cry4Ba) have been determined by X-ray crystallography (see **Figure 4**). They all share a common structure, which is composed of three domains. The N-terminal Domain I is composed of a central hydrophobic α5 helix, which is surrounded by six amphipathic helices to form a seven α-helix bundle. This domain is presumed to have a major role in pore formation, through insertion of some or all of those helices into the cell membrane. This assumption is based on the structural similarities with other PFTs like colicin Ia [**viii,xviii**]. Domain II is made up of three anti-parallel β-sheets. It is similar in structure to sundry carbohydrate-binding proteins like vitelline and the lectin jacalin, and so is assumed to be responsible for binding to the receptors of the gut cell membrane. Domain III is a tightly packed β-sheet sandwich that postulated to protect the C- terminal end of the active toxin from further cleavage after proteolytic activation by gut proteases [**xviii**-**xxi**].
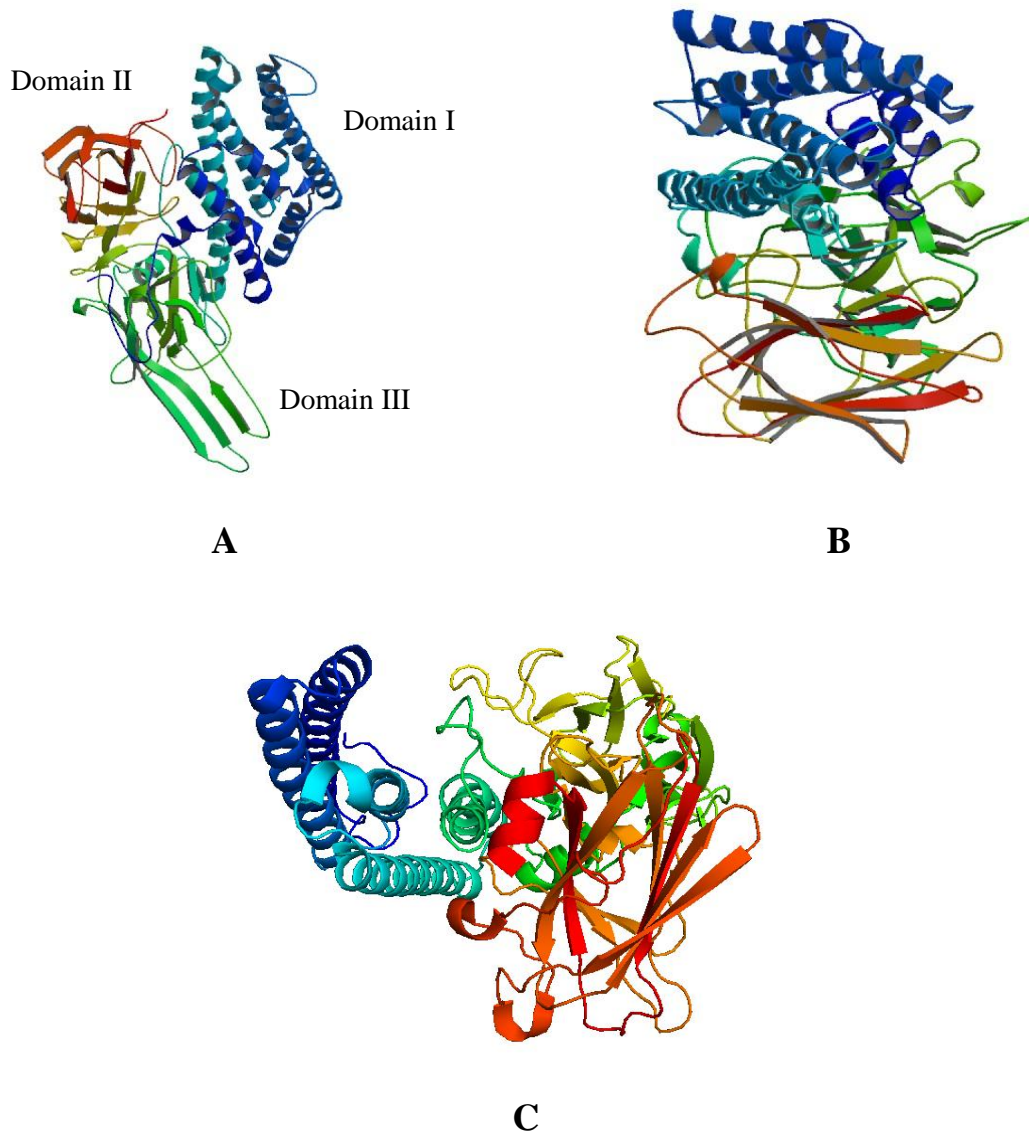
Figure 4 Ribbon representation of various cry family crystal structures. A: **Cry2Aa** (PDB entry 1I5P) crystal structure **[xix]** ; B : **CryIA(a)** (PDB entry 1CIY) **[xx]** ; C: **Cry4BA** (PDB entry 1W99) **[xxi]**. These structures were rendered from PDB records using Pymol **[xxxiv]**.

Table 1: Cry family and subgroups

Crystal type	subgroups	Protein size(kDa)
cry I	A(a), A(b), A(c), B, C, D, E, F, G.	130-138
cry II	A, B, C.	69-71
cry III	A, B, C.	73-74
cry IV	A, B, C, D.	73-134
cry V-IX	N/A	35-129

1.2.1.2 Cyt toxins:

The *cyt* δ-endotoxin form a small family of nine known members. They are structurally related to a cardiotoxic PFT called volvatoxin A2, which is produced by the straw mushroom *Volvariella volvacea* **[xxii]**. They have a molecular mass of around 25 kDa in their active form **[xxiii]**. These toxins have a single α-β domain comprising of two outer layers of α-helix hairpins wrapped around a β-sheet.

The *cyt* δ-endotoxins are highly specific for the larvae of dipterans, that is mosquitoes and black flies, although they are broadly cytolytic *in vitro*. They can insert into pure liposomal lipid bilayers without any need for a protein co-factor as receptor mediated mechanism for insertion **[xxiv]**. Like the *cry* toxins, the *cyt* toxins undergo the same steps of solubilization, proteolytic activation and membrane insertion. So far, six *cyt* δ-endotoxins have been sequenced and characterized, including Cyt1Aa (previously CytA) and Cyt2Aa (previously CytB) **[xxv]**. Both

Cyt1Aa and Cyt2Aa have been sequenced and characterised by Koni and Ellar **[xxv]**. Cyt1Aa has 249 amino acid residues and Cyt2Aa has 259 amino acid residues. They share 39% sequence identity and have the same tertiary structure.

1.2.2 Mode of action of *Bt* toxins

The *cry* toxins from different strains of *Bacillus thuringiensis* have similar modes of action and directly cause death of the insects. This mode of action involves the solubilization of the δ-endotoxin inclusion crystals in the alkaline mid-gut juice of the insect, proteolytic activation by mid-gut proteases of the insects, binding of activated *cry* toxins to specific receptors on the surface of the mid-gut epithelia, partial or complete membrane insertion and pore formation. The *cyt* toxins share the same mode of activation and mechanism of action, except that the membrane binding of *cyt* toxins does not require receptors. Moreover, while *cyt* toxins are widely assumed to act through the formation of discrete pores **[xxxviii, xli]** an alternative, detergent-like mechanism of action has also been advocated **[xxvi, 41]**.

1.2.3 Protoxin solubility

Bacillus thuringiensis δ-endotoxins are retained and stored inside the spores as inactive protoxin molecules, which are tightly packed inside crystalline inclusion bodies. The structure of these crystals is stabilized by intermolecular disulphide bridges **[xxvii]** and by intramolecular salt bridges that makes the toxin inclusion insoluble at neutral pH **[xviii].** However, the inclusion

crystals dissolve at an alkaline pH of 10.5-13. The pH dependence of solubility explains why the *Bacillus thuringiensis* δ-endotoxin inclusions are toxic to insects but not humans: An alkaline pH prevails in the mid-gut juice of the insects, in contrast to the acidic nature of the stomach juice of humans.

1.2.4 Protoxin activation

The solubilized protoxin undergoes proteolytic activation by the mid-gut proteases of the insects [v]. The activation usually involves proteolytic removal of a number of amino acids from both the N-terminal and C-terminal ends. The number of removed amino acids is variable according to the type and nature of each δ-endotoxin. For the *cry* toxins like Cry1, Cry4A and Cry4B, 3-70 amino acids are usually removed from the N-terminus during activation, while up to about half of the molecule may be removed from the C-terminus to activate the toxin [xxviii]. Unlike *cry* toxins, only few amino acids are removed from both N-terminal and C-terminal ends by proteases to activate the toxin. For example, 15 amino acids residues from the C-terminus and 32 amino acids residues from the N-terminus will be removed from the Cyt2Aa protoxin by proteolysis for the purpose of activation [xxiv,xxv].

1.2.4.1 Receptor binding

Activated *cry* toxins bind to specific receptors on the epithelial cell membrane of the insect. Binding is mediated by domains II and III [xxix]. Unlike *cry* toxins, no receptors have been

identified for the *cyt* family. It is assumed that this group of toxins does not need any specific receptors to exert their action **[v]**.

1.2.4.2 Pore formation

Both *cry* and *cyt* toxins are assumed to form oligomeric pre-pore structures containing several monomeric activated molecules prior to membrane insertion **[v]**. After insertion, the resulting pores cause colloidal osmotic lysis of the cells in the mid-gut, which leads to an irreversible arrest of gut movement, and the insect stops feeding. Once the insect's digestive activity has been disrupted, the Bt spores may germinate, then reach the hemolymph and cause septicaemia followed by death of the insect **[xxiv]**. In the case of *cyt* toxins, an alternative mechanism of membrane damage has been proposed. Instead of the formation of discrete pores, *cyt* toxins may cause rupture of the cells by a detergent-like mode of action, similar to the mode of action of defensins and other antimicrobial peptides **[xxx,xxxi]**. Briefly, according to this hypothesis, the toxin monomers adsorb to the membrane surface and then haphazardly aggregate into large carpet-like structures. The molecules insert only shallowly into the head group layer of the lipid bilayer. The distension of the head group layer disrupts the regular packing of the lipid molecules in the bilayer, causing membrane destabilization and disruption. This results in the leaking of cytoplasm and finally cell disintegration.

1.3 Cyt2Aa1

The Cyt2Aa1 toxin (PDB accession number 1CBY), previously known as CytB, is produced *in vivo* as a 29 kDa protoxin, which is proteolytically cleaved at both ends by gut proteases to generate the active 21-23 kDa toxin **[xxxii]**. The crystal structure of Cyt2Aa1 toxin in its monomer form is composed of a single domain of α/β architecture with two outer layers of α-helix wrapped around a mixed β-sheet (see **Figure 5** and **Table 2**). Cyt2Aa1 is produced in the protoxin form as a dimer which is cross-linked by the interlaced N-terminal strands from both monomers in a continuous, 12-stranded β-sheet (see

Figure 6) **[xiv,xxiv,xxxiii]**. Proteolytic activation by proteinase K cleaves the interlaced β-strands, removing 32 amino acid residues from the N-terminus end and 15 amino acid residues from the C-terminus to expose the three-layered core **[xxxiii,xxiv,xxv]**. In contrast to *cry* toxins, *cyt* toxins do not bind to protein receptors but interact directly with membrane lipids **[xiv,xxiv,xxxi]**.
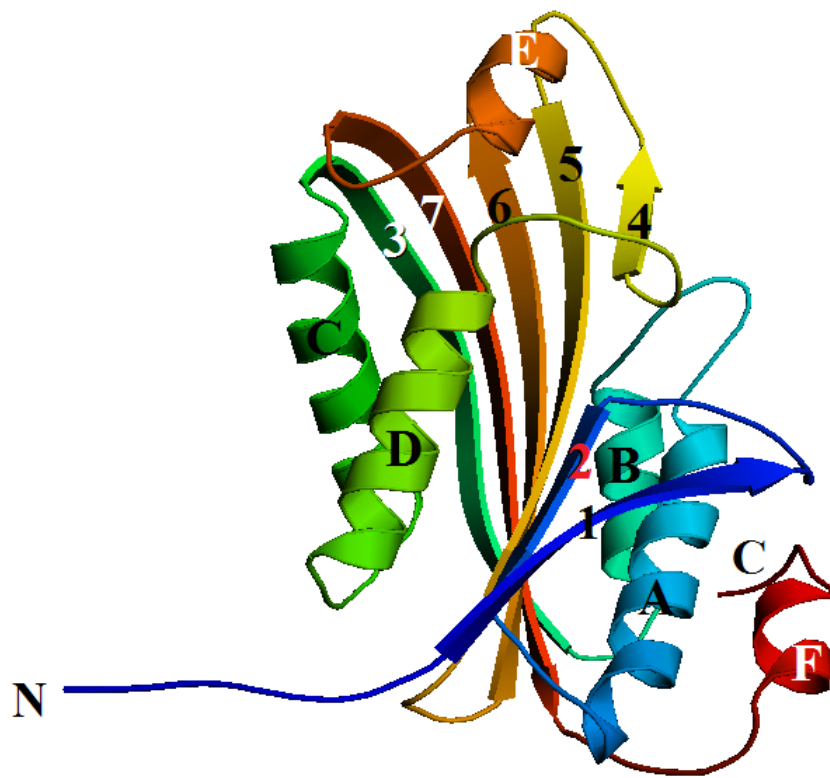
Figure 5 Cyt 2Aa1toxin consists of two outer alpha helix hairpins (helices A-B and C-D) surrounding a core of mixed beta-sheet (strands 1 to 7). α-Helices are marked by letters, and β strands are numbered. This structure was rendered from the PDB record 1CBY using Pymol **[xxxiv]**.
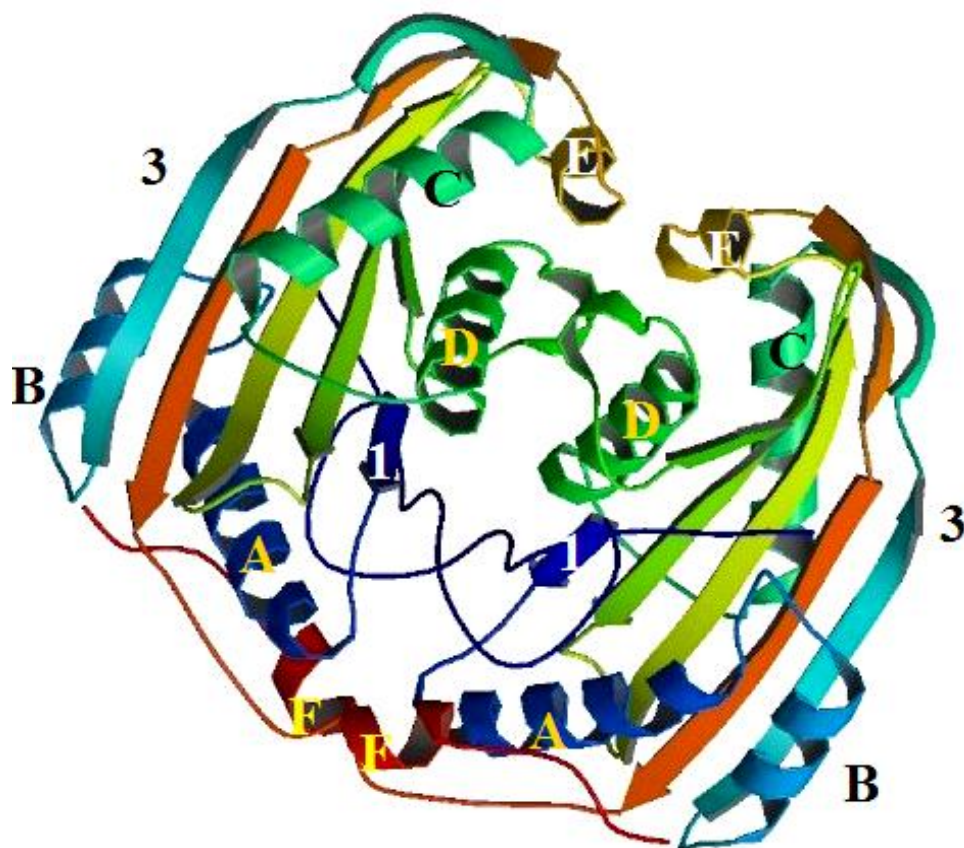
Figure 6 : Ribbon drawing for Cyt2Aa1 protoxin dimer. This structure was rendered from PDB records 1CBY using Pymol software **[xxxiv]**.

Table 2 Secondary structure of Cyt2Aa1

α-Helix	Residues	β-Strand	Residues
A	54-63	1	28–36
B	77-84	2	44–48
C	107–122	3	90–106
D	129–140	4	155–158
E	199–202	5	165–175
F	233–237	6	183–195
		7	210–225

1.4 Aim of the work

To date, the tertiary structure of Cyt2Aa1 toxin is well known **[xiv].** However, its mechanism of action is still controversial, and the structure of the membrane-associated form is unknown. The goal of this work is to characterize the mode of membrane permeabilization by Cyt2Aa1 and the structural changes that accompany its activity.

One reason for the limited knowledge is the lack of a reliable and efficient system for recombinant expression of Cyt2Aa1. So, the initial goal was to develop a reliable system for cloning, production and purification of the recombinant Cyt2Aa1 toxin.

In previous work with Cyt2Aa1 toxin, the toxin had been obtained by direct extraction of Cyt2Aa1 crystals from *Bacillus thuringiensis* subspecies *kyushuensis* after sporulation. Another study has used a *Pichia pastoris* expression system, but the yield of active toxin was relatively low **[xxxv]**. In this project, we have developed an improved *Escherichia coli* expression system that achieved a higher yield of the functionally active Cyt2Aa1 toxin. Further functional characterization experiments had been done to test the activity of the functionally active Cyt2Aa1 toxin.

We propose to investigate the intermediary model of Cyt2Aa1 toxin prior to the pore formation and whether or not the toxin penetrates into membranes. To this end, we have constructed two Cyt2Aa1 single cysteine mutants V186C and L189C that can be labelled with polarity-sensitive fluorescent dyes such as nitrobenzoxadiazole (NBD) and use them in fluorescence experiments to study the oligomerization and insertion.

Finally, we have established a model system (liposomes) to characterize the activity of Cyt2Aa1 toxin and to use it in pursuing further fluorescence experiments.

2   Materials and Methods

2.1   Cloning

The sequence of the wild type Cyt2Aa1 toxin was synthesized and verified by IDT integrated

DNA technologies, Inc. (as shown in **Figure 9**). The IDT codon optimization tool is designed to

use parameters that exclude codons used less than 10% per amino acid. Thus the codon

optimization tool has a 10% usage threshold. For the codons used at or above 10%, the

optimization algorithm incorporates all of these codons with a bias toward more frequent codons.

The synthetic gene was codon-optimized for *E.coli. Bgl*II and *Xho*I cleavage sites were been

introduced at the two ends of the gene for cloning purposes. The synthetic gene was re-cloned

into the pET30a+ expression vector, which supplies a His-Tag.

The vector pUC57-Cyt2Aa1 insert and the plasmid pET-30a(+) were double-digested with the

restriction enzymes *Bgl*II and *Xho*I. The digested DNA fragments were separated by gel

electrophoresis and the Cyt2Aa1 DNA fragment and *Bgl*II-*Xho*I-digested pET-30a(+) fragment

were extracted and ligated to each other.

Cyt2aa-wt

M13 (-20) Forward

M13 (-27) Reverse

pUC57 : Cyt2aa-wt
Ref ID: 34239924

2,173,782.7 g/mole
3518 bp

pMB1 Origin

bla (ApR)
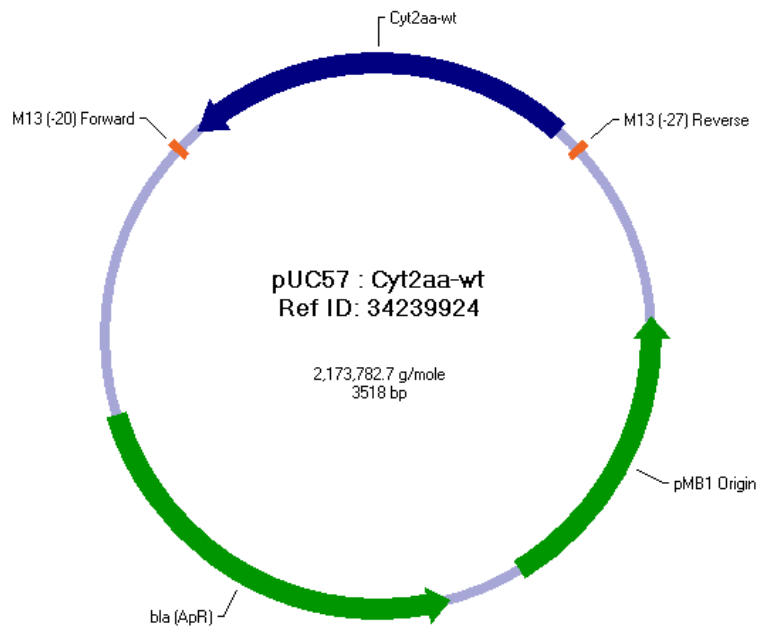
**Figure 7** : Cyt2Aa1 gene in pUC57 vector. This plasmid was obtained from IDT-DNA.
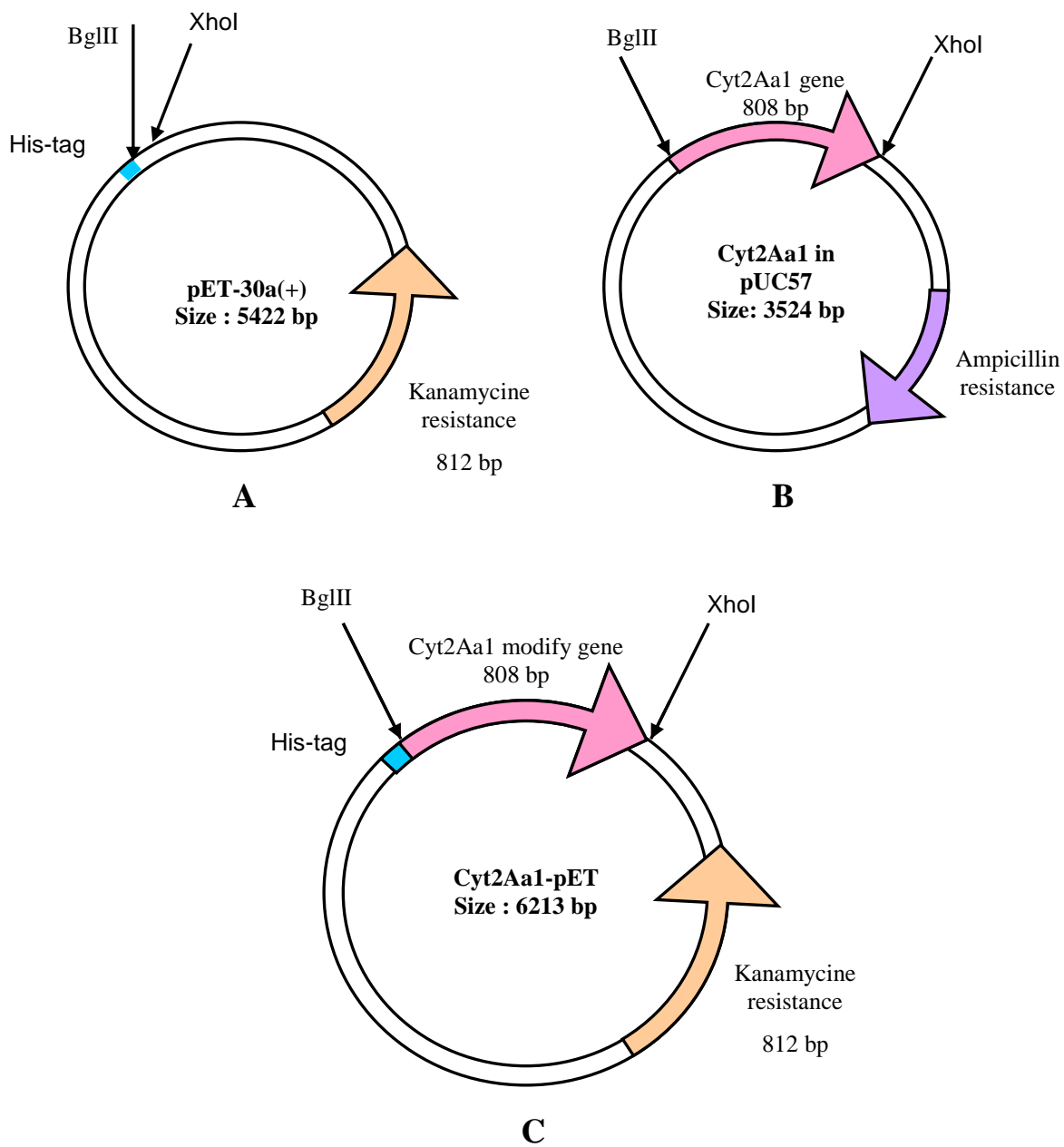
Figure 8: Map of the plasmids pET-30a(+) (A), Cyt2Aa1 in pUC57(B) and Cyt2Aa1-pET, in which the modified Cyt2Aagene was inserted into the pET-30a(+) vector (C).

```
native      ATGTATACTAAAAATTTTAGTAATTCCAGAATGGAAGTAAAAGGTAATAACGGCTGTTCT
synthetic   ATGTACACGAAGAATTTCTCCAACTCTCGCATGGAGGTTAAAGGTAACAACGGCTGTTCT
                 ^   ^   ^     ^^^^  ^   ^^ ^       ^   ^        ^

native      GCACCTATTATTAGAAAACCATTTAAACATATTGTATTAACGGTTCCATCCAGTGATTTA
synthetic   GCGCCGATCATTCGTAAACCGTTCAAGCACATCGTACTGACCGTTCCGTCTTCTGACCTC
              ^   ^   ^    ^ ^      ^   ^  ^   ^   ^   ^  ^        ^  ^^^    ^^

native      GATAATTTTAATACAGTCTTTTATGTACAACCACAATACATTAATCAGGCTCTTCATTTA
synthetic   GACAACTTCAACACGGTTTTCTACGTTCAGCCGCAGTACATCAACCAGGCCCTGCACCTG
              ^   ^   ^   ^   ^  ^   ^   ^   ^   ^   ^      ^   ^      ^   ^   ^^

native      GCAAATGCTTTTCAAGGGGCTATAGACCCACTTAATTTAAATTTCAATTTTGAAAAGGCA
synthetic   GCGAATGCGTTCCAAGGTGCCATCGATCCGCTGAACCTGAACTTTAACTTCGAGAAAGCG
                ^       ^   ^      ^   ^   ^   ^   ^   ^^   ^   ^   ^   ^   ^

native      CTCCAAATTGCAAATGGTATTCCTAATTCTGCAATTGTAAAAACTCTTAATCAAAGTGTT
synthetic   CTGCAGATTGCGAACGGTATCCCGAATTCTGCGATCGTTAAGACCCTGAACCAGTCCGTG
                ^   ^     ^   ^      ^   ^        ^   ^   ^   ^   ^   ^   ^   ^^^^

native      ATACAGCAAACAGTTGAAATTTCAGTTATGGTTGAGCAACTTAAAAAGATTATTCAAGAG
synthetic   ATCCAGCAAACGGTGGAGATCAGCGTCATGGTGGAACAGCTGAAGAAAATTATCCAAGAA
                ^       ^   ^   ^   ^^^^  ^      ^   ^   ^   ^   ^   ^       ^

native      GTTTTAGGACTTGTTATTAACAGTACTAGTTTTTGGAATTCGGTAGAAGCTACAATTAAA
synthetic   GTTCTCGGCCTCGTCATCAACTCTACCTCTTTTTGGAACTCTGTTGAGGCAACGATCAAA
                 ^ ^   ^   ^   ^   ^   ^^   ^^^          ^   ^   ^   ^   ^   ^   ^

native      GGCACATTTACAAATTTAGACACTCAAATAGATGAAGCATGGATTTTTTGGCATAGTTTA
synthetic   GGTACTTTCACCAACCTGGATACCCAGATCGACGAAGCGTGGATCTTCTGGCACTCTCTG
                ^   ^   ^   ^   ^^ ^   ^   ^   ^   ^   ^      ^   ^   ^      ^^^ ^

native      TCCGCCCACAATACAAGTTATTATTATAATATTTTATTTTCTATTCAAAATGAAGATACA
synthetic   TCTGCCCACAACACCAGCTACTACTACAACATTCTGTTCAGCATCCAGAATGAGGACACG
                ^         ^   ^   ^   ^   ^   ^   ^   ^   ^^  ^^^^  ^   ^      ^   ^

native      GGTGCAGTTATGGCAGTATTACCTTTAGCATTTGAGGTTTCTGTGGATGTTGAAAAACAA
synthetic   GGCGCAGTCATGGCGGTTCTGCCGCTGGCGTTTGAAGTGAGCGTCGATGTTGAGAAGCAG
                ^       ^      ^   ^^ ^   ^^ ^   ^          ^   ^^^^  ^         ^   ^

native      AAAGTATTATTCTTTACAATAAAAGATAGTGCACGATATGAAGTTAAAATGAAAGCTTTG
synthetic   AAGGTCCTGTTCTTCACCATCAAGGACTCCGCTCGCTACGAGGTAAAAATGAAGGCGCTC
                ^ ^^ ^      ^   ^   ^   ^   ^^^^  ^   ^   ^   ^   ^         ^   ^^

native      ACTTTAGTTCAAGCTCTACATTCCTCTGATGCCCCAATTGTAGATATATTTAATGTTAAT
synthetic   ACCCTGGTCCAAGCTCTGCACTCTTCTAACGCGCCAATCGTCGACATTTTCAACGTCAAC
                ^^ ^   ^          ^   ^   ^    ^ ^   ^      ^   ^   ^   ^   ^   ^

native      AACTATAATTTATACCATTCTAATCATAAGATTATTCAAAATTTAAATTTATCGAAT
synthetic   AACTACAACCTGTACCACAGCAACCACAAGATCATCCAAAATCTCAACTTAAGTAAC
                 ^   ^^ ^       ^^^^  ^   ^       ^   ^       ^   ^   ^   ^^^   ^
```

Figure 9: Sequence alignment of native and synthetic Cyt2Aa1 gene. The bases that were substituted in the synthetic gene are highlighted by the ^ symbols.

The synthetic Cyt2Aa gene was cut from the pUC57 vector and cloned into the pET-30a(+) plasmid, which contains a His-Tag and has a kanamycin resistance gene. The cloning procedure was as follows:

The vector pUC57-Cyt2Aa1 insert and the plasmid pET-30a(+) were double-digested with the restriction enzymes *Bgl*II and *Xho*I (MBI Fermentas,**Table 3**.A) and incubated for 3 hours at 37°C. The digested DNA fragments were then separated by electrophoresis on a 0.8% agarose gel and the desired DNA fragment recovered using the QIAquick® Gel Extraction Kit (Quiagen) according to the manufacturer's procedure.

The Cyt2Aa1 gene was ligated into BglII-XhoI-digested pET-30a(+) (ligation, see **Table 3**.B). The ligation mixture was then transformed into *E. coli* XL1Blue cells by heat shock. The plasmid carrying the insertion was then purified and double-digested with the restriction enzymes *Bgl*II and *Xho*I. The purified plasmid and the double digested one were then applied into an electrophoresis on a 0.8 % agarose gel to visualize the generated product, and the sequence of the recombinant Cyt2Aa1 gene confirmed by DNA sequencing. The map of the Cyt2Aa1-pET plasmid is shown **Figure 8C** and the final sequence of the Cyt2Aa1 gene is shown in Figure 9. For protein expression, the plasmid was then transformed by electroporation into *E. coli* BL21(DE3) cells.

Table 3 : Restriction and Ligation mixtures

DNA	7 µl		10x buffer for T4 DNA	2µl
Autoclaved water	11 µl		Cyt gene	10µl
*Xho*I	1 µl		pET linearised	5µl
*Bgl*II	1 µl		autoclaved water	2µl
10x O$^+$ Buffer	2 µl		T4 DNA ligase	1µl
A			B	

A: Digestion mixture. *Bgl*II and *Xho*I and O$^+$ Buffer were ordered from Fermentas. B: Ligation mixture (incubated 2 hours at room temperature). 10 x buffers for T4 DNA ligase and T4 DNA ligase was ordered from Fermentas.

2.2 Site-Directed mutagenesis

Site-directed mutagenesis was done to substitute valine at position 186 and leucine at position 189 with cysteine in the Cyt2Aa1 toxin (see **Figure 10**). The mutation had been made by using designed primers (see **Table 4**), which were ordered from Sigma Genosys (Oakville, ON). KOD DNA polymerase (Novagen Inc, Madison, WI) was used as described by the manufacturer. Briefly, The double-stranded target plasmid DNA of Cyt2Aa1 in pET-30a(+) vector was mixed with the PCR mixture (see **Table 5**) and then the reaction mixture was incubated at an initial hold temperature of 95 °C for 2 min followed by 18 cycles of 95 °C for 30 s, 55 °C for 30 s, 72 °C for 60 s, and finally hold at 74 °C for 10 min. PCR products were run on a 0.8% agarose gel stained with ethidium bromide (0.7 μg/ml) for confirmation. Both PCR products were digested with the restriction enzyme Dpn1 before transformation to digest template DNA. The new V186C and L189C mutants were verified by sequencing (Mobix Lab, McMaster University, Hamilton, ON).

Table 4   The position of amino acid substitution and the primer sequences used for mutation

Oligonucleotide	position of amino acid substitution	Sequence (5'→3')	Length (Bases)	Tm °C
Sense (5') primer 1	V186C	GCAGTCATCGCG<u>TGT</u>CTGCCGCTGGCG	27	86.4
Anti-Sense (3') primer 1	V186C	CGCCAGCGGCAG<u>ACA</u>CGCGATGACTGC	27	86.4
Sense (5') primer 2	L189C	GCGGTTCTGCCG<u>TGC</u>GCGTTTGAAGTGAGCG	31	87.6
Anti-Sense (3') primer 2	L189C	CGCTCACTTCAAACGC<u>GCA</u>CGGCAGAACCGC	31	87.6

Table 5 PCR reaction mixture

Component	Volume	Final concentration
10 X Buffer for KOD XL DNA Polymerase	5 µl	1X
Sense (5') primer	1.25µl	5 pmol/ µl
Anti-Sense (3') primer	1.25µl	5 pmol/ µl
dNTP	5 µl	0.2 mM
Cyt2Aa1 template DNA	1 µl	2 ng/ µl
KOD XL DNA Polymerase (2.5 U/ µl)	1 µl	0.05 U/ µl
PCR Grade Water	36.5 µl	
Total reaction volume	50 µl	

2.3   Preparation of competent cells and transformation

2.3.1 Heat shock

E. coli XLI-Blue competent cells for heat shock transformation were prepared according to the procedure obtained from "Short protocols in molecular biology"[xxxvi]. Briefly, 200 mL of LB medium (5 g/L NaCl, 10 g/L Bio-Trypton, 5 g/L Yeast extract) were inoculated with 2 mL of overnight culture and grown to an $O.D._{600}$ of 0,3 to 0,4 with vigorous shaking (200 rpm) at 37°C.

The bacterial culture was then centrifuged at 5000 rpm for 10 minutes at 4°C. The supernatant was discarded and the cells were re-suspended in 1mL of LB and 1mL of 2xTSS buffer (18 % (w/v) PEG 3350, 45.5 mM $MgCl_2$ and 10 % (v/v) DMSO) and stored at -80°C as 100µL aliquots.

100µL of heat chock competent *E. coli* XL1-Blue cells were mixed with an appropriate amount of DNA (1 to 5 µL) and incubated on ice for 45 minutes. Then, the cells were heat shocked by placing tubes 45 seconds in 42°C water bath. The cells were then incubated 2 minutes in the ice, afterwards incubated in 1mL of LB at 200 rpm and 37°C in the absence of antibiotic. Finally, 100µL of the incubated mixture was plated on a LB agar plate containing 30 mg/L kanamycin. The plates were incubated overnight at 37°C.

2.3.2 Electroporation

E. coli BL21(DE3) electrocompetent cells were prepared following the protocol from "Short protocols in molecular biology"xxxvi. Briefly, 500 mL of LB medium (5 g/L NaCl, 10 g/L Bio-Trypton, 5 g/L Yeast extract) in a 2L flask were inoculated with 2,5mL of overnight culture and grown to an $O.D._{600}$ of 0,5 to 0,6 with shaking (300 rpm) at 37°C. The cells were chilled in an ice-water bath 10 to 15 minutes and transferred to a 1 L pre-chilled centrifuge bottle. The bacterial culture was then centrifuged at 5000 x g for 20 minutes at 2°C. The supernatant was discarded and the cells were resuspended in 5 mL ice-cold water. 500 mL of ice-cold water was then added and mixed to the pellet and then centrifuged at 5000 x g for 20 minutes at 2°C. This step was repeated once. The supernatant was discarded and the pellet was resuspended by

swirling in remaining liquid. 40 mL of ice-cold 10 % glycerol was added, mixed and centrifuged 10 minutes at 5000 x g and 2°C. The supernatant was discarded, the pellet volume was estimated and an equal volume of ice-cold 10 % glycerol was added to resuspend the cells. Aliquot of 40 µL were added into prechilled Eppendorf tubes, froze on dry ice and store on - 80 °C.

40 µL of eletro-competent *E. coli* BL21(DE3) cells were mixed with 0.7 µL of DNA, then transferred to a 0.1 cm electroporation cuvette and subjected to electroporation at 1.8 kV. After eletroporation, cells were transferred to 1mL of SOC solution (20 g/L trypton , 5g/L yeast extract supplemented with 10 mM NaCl, 20 mM KCl, 10 mM $MgCl_2$, 10 mM $MgSO_4$) and shaken at 200 rpm for 1h at 37°C. 100 µL of the above culture were plated on a LB agar plate with 30mg/L kanamycin. The plate was incubated overnight at 37°C.

2.4 Protein expression and purification

2.4.1 Induction

A single colony of BL21(DE3) containing Cyt2Aa1-pET gene was grown at 37°C overnight in 50mL of 2xYT medium (5 g/L NaCl, 16 g/L tryptone, 10 g/L yeast extract) containing 30 mg/L kanamycin. The overnight culture was then added to 2 L of 2xYT medium containing 30 mg/L kanamycin. The culture was shaken vigorously (200 rpm) at 37°C until the OD_{600} reached 0.6. Then, the BL21(DE3) bacteria were induced with 1mM IPTG (isopropyl β-D-thiogalactoside) then shaken slowly (150 rpm) overnight at 25°C.

2.4.2 Protein purification

Cells were harvested by centrifugation 5 min at 8,000 rpm. The cell pellets were resuspended in binding buffer (Tris 20 mM, NaCl 150 mM, pH 8.0). The cells were then lysed using an emulsifier (Aventin Emulsiflex-C5) at 17,500 psi and the insoluble cell remnants were sedimented by centrifugation at 20,000 rpm for 30 min at 4°C. The protoxin contained in the supernatant was purified by metal-chelating chromatography on a pre-packed column of Ni-NTA agarose (Qiagen) and then eluted from the column with a linear gradient of imidazol (10 mM − 450 mM) in binding buffer using (Bio-Rad Bio Logic LP) instrument. To purify the protoxin contained in the pellets, the latter were washed by vortexing (Vortex-Genie 2 from Scientific industries) with 150 ml of ice-cold distilled water and then centrifuged at 20,000 rpm for 10 min at 4°C. The process of washing was repeated for five times. The pellets were then resuspended in 15 ml of Tris buffer (Tris 10 mM, NaCl 150 mM, pH 7.4) and stored   at −80 °C. After thawing, the pellets were solubilized by incubation for 1 h at 37 °C in 50 mM Na_2CO_3, pH 10.5. The solubilized toxin was separated from remaining insoluble material by centrifugation at 13,000 g for 10 min and stored at −20 °C. SDS-PAGE was performed on the toxin obtained from both supernatant and the cell pellets.

2.5   Proteolytic activation

The activation of the protoxin of Cyt2Aa1 wild type and the V186C L189C mutants was done by addition of proteinase K (1% w/w) and incubation at 37 °C for 1 h **[xxv].**

2.6   Activity assays

Lysis of red blood cells and calcein release assay were done to measure the activity of the proteolytically activated Cyt2Aa1 wild type and V186C, L189C toxin mutants.

2.6.1   Lysis of RBCs

Sheep red blood cells (Cedarlane®, Hornby, Ontario, Canada) were washed four times with hemolysis buffer (10 mM Tris-HCl, 150 mM NaCl, pH 7.4) by centrifugation. The washed RBCs were resuspended in hemolysis buffer to a final concentration of 0.2% (v/v). 50 μL of cell suspension was added to the wells of a microtiter plate containing two fold serial dilutions of activated Cyt2Aa1 toxin in 150 μL of the former buffer and incubated for 30 min at 37°C. Hemolysis was detected by measuring the absorbance for the decrease in turbidity (A_{600}) using a 96-well plate reader (Spectramax 190, Molecular Devices, Sunnyvale, CA).

2.6.2 Calcein release assay

All lipids (cholesterol, DMPC and DMPG) were purchased from Avanti Lipids (Alabaster, AL). The lipids had been dissolved in chloroform and mixed in various molar ratios (see **Table 6**). The lipid solutions had been dried down under a stream of nitrogen in a round-bottom flask for 5 min and then dried under vacuum for an additional 4 h at least to remove any residual traces of chloroform. The dried lipids were re-suspended by sonicating for 10 min with 1.5 ml of HEPES buffer (10 mM Hepes, 150 mM NaCl, pH 7.4) containing 50 mM calcein at room temperature. The resulting suspensions of multilamellar lioposomes were sized down to unilamellar liposomes using a liposome extruder (Northern Lipids, 78 Vancouver, British Columbia, Canada) by extruding 10 times via a 100-nm polycarbonate membrane filter (Whatman Millipore, USA). Subsequently, the liposome suspension was purified from non-encapsulated calcein dye by gel filtration on a Bio-Gel$^®$ A-1.5m Gel (Bio-Rad Laboratories; CA) column (1 cm $\times$ 20 cm) which was equilibrated with Hepes buffer. The liposomes with calcein entrapped inside were mixed with various concentrations of activated Cyt2Aa1 toxin in HEPES buffer and incubated at room temperature for 5 min. The samples were diluted with the same buffer, and calcein fluorescence intensity was measured immediately (excitation, 470 nm; emission, 512 nm). The amount of calcein released was calculated by subtracting the fluorescence intensity of a control sample incubated without toxin from liposome samples incubated with Cyt2Aa1 activated toxin. 100% release was obtained from a liposome sample lysed with Triton X-100 to a final concentration of 0.1%. The permeability of liposome membranes was calculated using the following formula:

$P= (F_s - F_0) / (F_\infty - F_0)$

Where P is the fraction of liposomes permeabilized,

F_S is the calcein fluorescence intensity of the liposome sample incubated with Cyt2Aa1 toxin,

F_0 is the fluorescence of liposomes incubated without the toxin and

F_∞ is the fluorescence of a sample after lysis by Triton X-100.

Table 6 Lipid compositions of liposomes used in permeabilization assays

Type of lipid(s) used in liposomes preparation	Molar ratios
DMPC	100%
DMPC+ DMPG	60%+40%
DMPC+ cholesterol	90%+10%

3   Results

3.1   Cloning of the recombinant Cyt2Aa1 gene

The cloning of recombinant Cyt2Aa1 gene was accomplished. For confirmation, the Cyt2Aa1 gene was verified by sequencing both V186C and L189C mutants (Mobix Lab, McMaster University, Hamilton, ON).

3.2   Site- Directed mutagenesis

Both V186C and L189C mutants (see **Figure 10**) had been done successfully and verified by sequencing (Mobix Lab, McMaster University, Hamilton, ON).

3.3   Protein expression and purification

The protoxin contained in the supernatant was purified by metal-chelating chromatography on a pre-packed column of Ni-NTA agarose and then eluted from the column with a linear gradient of imidazol (10 mM – 450 mM) in binding buffer. The yield of the protoxin in the supernatant was relatively low (10mg/L) when compared with the protoxin contained in the pellets (0.4 g/L). To purify the protoxin contained in the pellets, the latter were washed as described in the Methods section. The pellets were solubilized by incubation for 1 h at 37 °C in 50 mM Na_2CO_3, pH 10.5. The solubilized toxin was separated from remaining insoluble material by centrifugation at 13,000 g for 10 min and stored at −20 °C. SDS-PAGE was performed on the protoxin obtained from the cell pellets (see **Figure 11, Figure 12**).
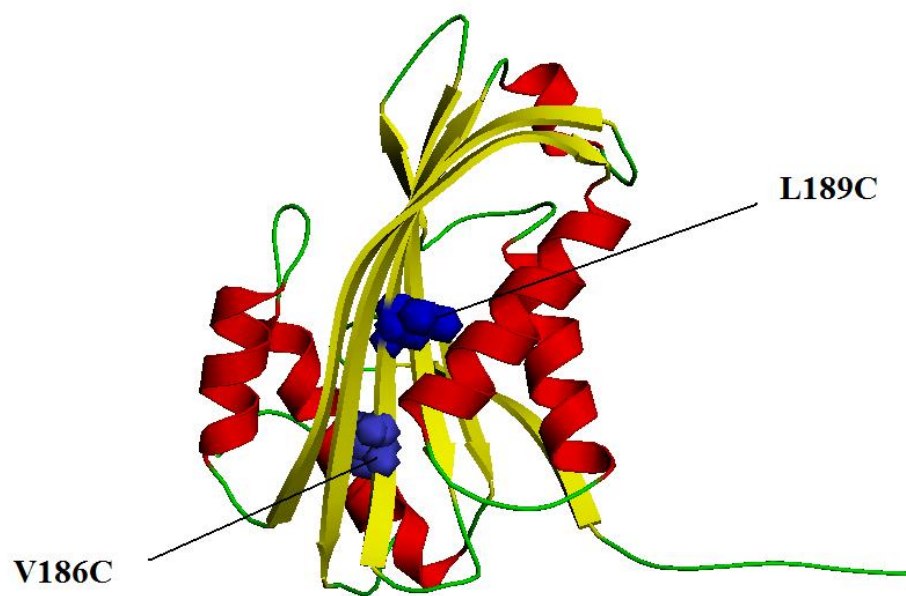
**Figure 10** Positions of V186C and L189C mutants. This structure was rendered from PDB record 1CBY using Pymol **[xxxiv]**.
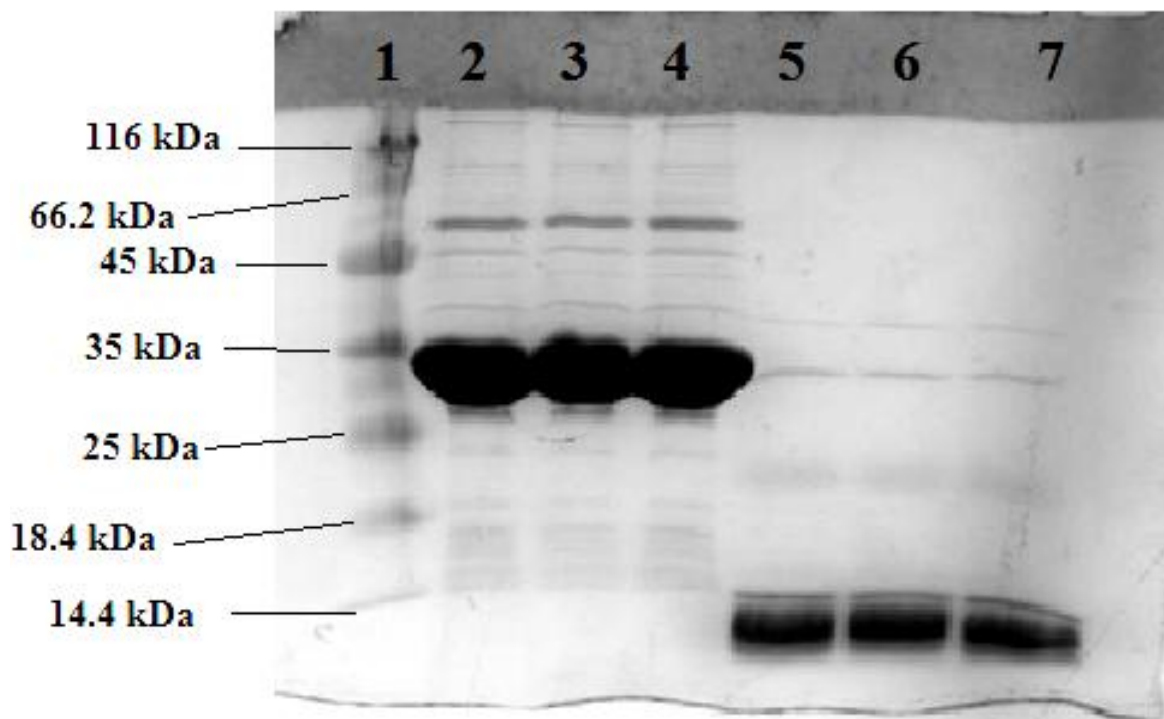
Figure 111 SDS 12%-polyacrylamide gel. 1: ladder ; 2,3,4: solubilized protoxin monomer (29 kDa) and solubilized protoxin Dimer   (58 kDa); 5,6,7: solubilized protoxin proteolized 1h at 37°C with 1% (w/w) proteinase K . proteinase K was not deactivated with PMSF before loading.
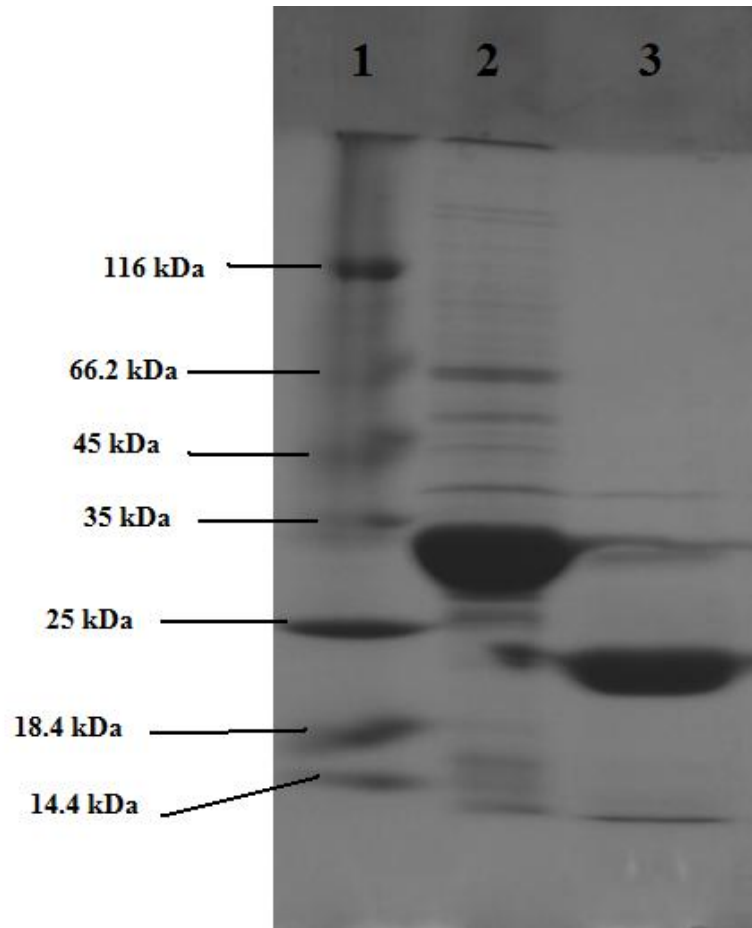
Figure 12 SDS 12%-polyacrylamide gel. 1: ladder ; 2: solubilized protoxin ; 3: solubilized protoxin proteolized 1h at 37°C with 1% (w/w) proteinase K ; proteinase K was deactivated with PMSF before loading.

3.4 Proteolytic activation

The protoxin obtained from the pellets was mixed with different amounts of proteinase K for proteolytic processing. The activity test for all variants of CytAa1 toxin (wild type, and mutants V186C and L189C) had given positive results (see **Figure 14**). It was therefore surprising that the activated toxin did not show a band as shown on the SDS PAGE **Figure 11**. We found that the reason for this phenomenon was the high stability and activity of proteinase K in the presence of SDS. This activity is such that during the electrophoresis experiment the enzyme digests the entire activated toxin, which is denatured by SDS. To solve this problem and make sure that we got the right activated protoxin, proteinase K was deactivated by adding PMSF (5mM) before denaturing the sample with SDS. With this precaution, the activated toxin is clearly shown as a clear band of ~ 23 kDa (see **Figure 12**).

More experiment were done to test the effect of the concentration of proteinase K and the duration of activation as well.

3.4.1 Effect of the concentration of proteinase K on proteolytic activation

Protoxin samples were incubated with 10%, 5%, 1%, 0.5%, 0.25% and 0.1% (w/w) proteinase K at 37 °C for 100 minutes. All protoxin samples were activated to a detectable degree. Protoxin samples that been incubated with concentrations less than 0.25 % (w/w) of proteinase K showed delayed proteolytic activation (see **Figure 13**). When proteinase K was deactivated with PMSF after 30 min, all samples showed the same degree of activity after 30 min as non-deactivated proteinase K samples, except with sample of 0.1% (w/w) proteinase K concentration (Data not shown).
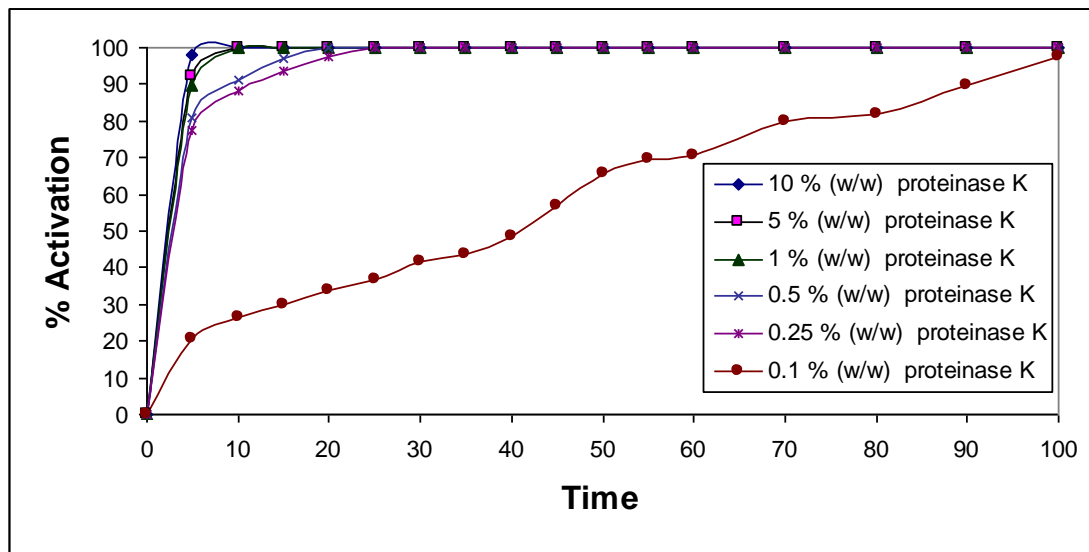
Figure 13 Hemolysis for Cyt2Aa1 wild type and mutants, 1 ml Cyt2Aa1 (2mg/ml) was mixed with different concentrations of proteinase K then 100 μl of Cyt2Aa1 (150 μg) was mixed with 100 μl of 1% (v/v) sheep RBCs in PBS, pre-incubated 37 °C. The samples were then incubated at room temperature. The extent of hemolysis was assessed every 5 min for 100 min by measuring the absorbance at 595 nm. The percentage of activation was then calculated using RBCs in PBS as the negative control and a sample of RBCs treated with 0.1% Triton X-100 as the positive control.

3.5 Hemolytic activity

To study the relationship between the concentration of Cyt2Aa1 and the hemolysis of RBCs, various concentrations of activated toxin were incubated with red cells, and the fraction of the remaining unlysed cells was measured by the absorbance at 595 nm after 30 minutes.

At concentrations greater than 135 µg/ml, the hemolytic activity decreases with decreasing concentration, which is what one would expect. Surpringly, however, at very high concentrations, the toxins also showed reduced activity (see **Figure 14**). Furthermore, the activity of the mutants was not the same as the wild type. The V186C mutant showed the highest activity, followed by the wild type toxin and the L189C mutant.
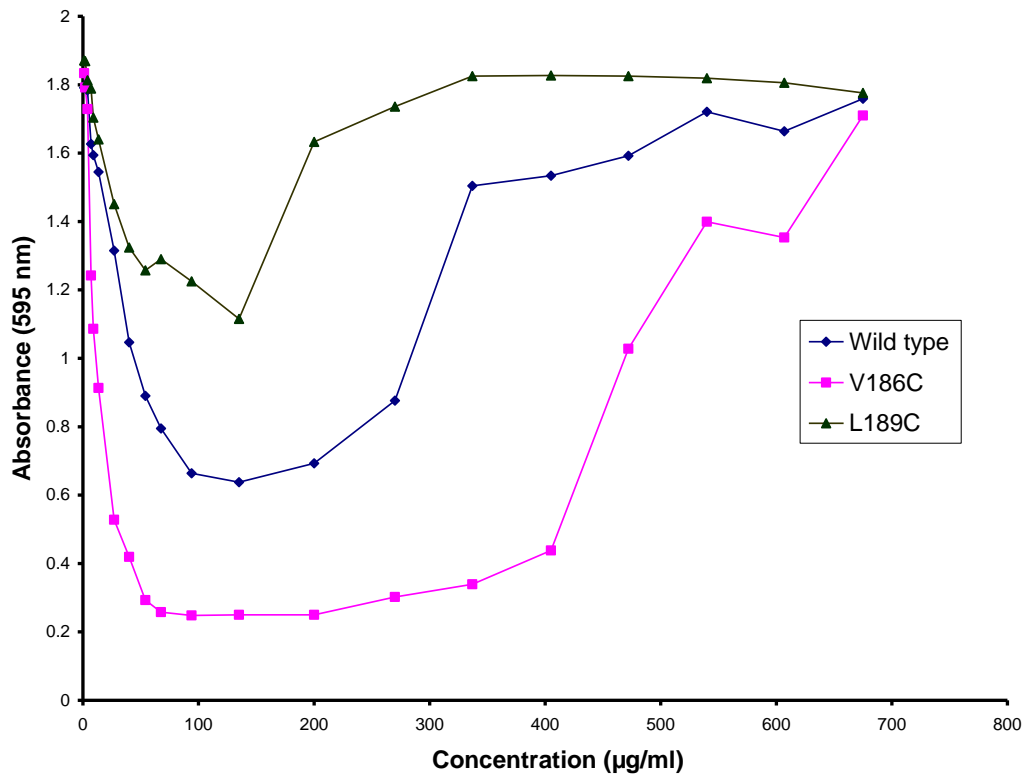
Figure 14 Dose–response curve of RBCs lysis by Cyt2Aa1. The turbidity of the samples (Absorbance from RBCs at 595 nm) was measured after 30 min of incubation at 37 °C using PBS as a blank and a sample of 1% sheep RBC treated with 0.1% Triton X-100 as the positive control.

3.6 Calcein release assay

DMPC, DMPC+ DMPG and DMPC+ cholesterol liposome containing calcein were prepared (see **Table 6**) and then incubated with different concentrations of toxin.

With DMPC liposomes, the maximal permeabilization did not occur at the highest toxin concentration, but rather at intermediate ones (see **Figure 16**). Further dilution caused the permeabilization to vanish. A similar behaviour was also observed with liposomes containing a mixture of DMPC and DMPG. DMPC+cholesterol liposomes did not show any noticeable permeability.
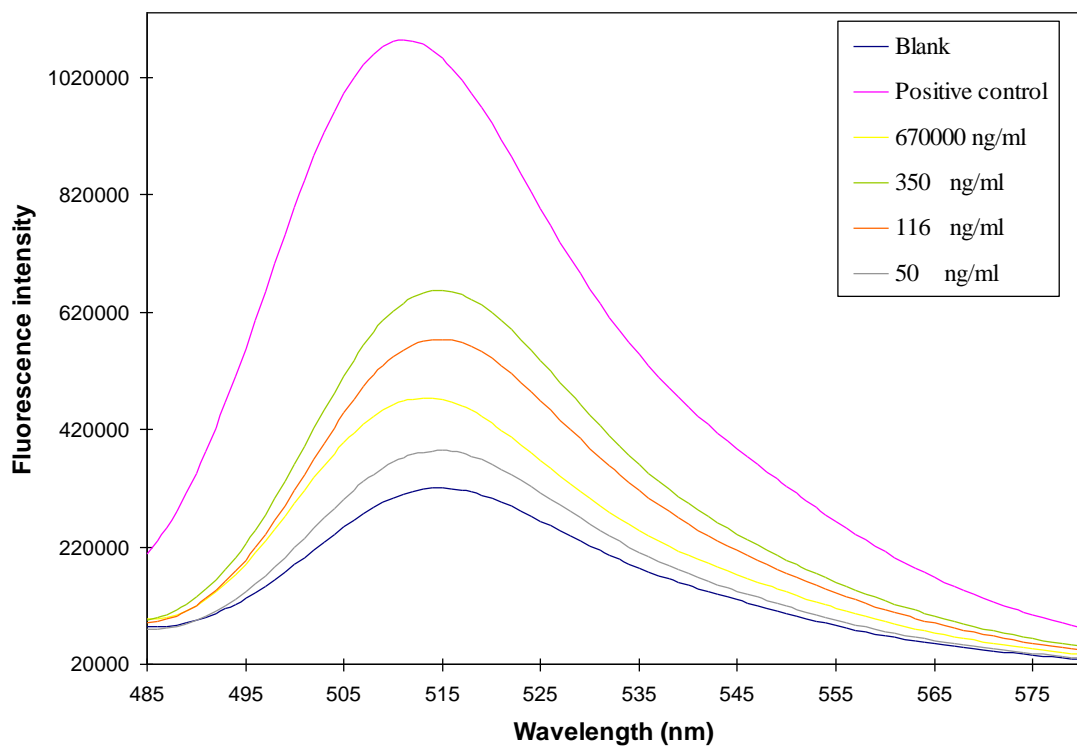
Figure 15 The emission spectra of DMPC+DMPG liposomes incubated with different concentrations of Activated Cyt2Aa1 toxin.
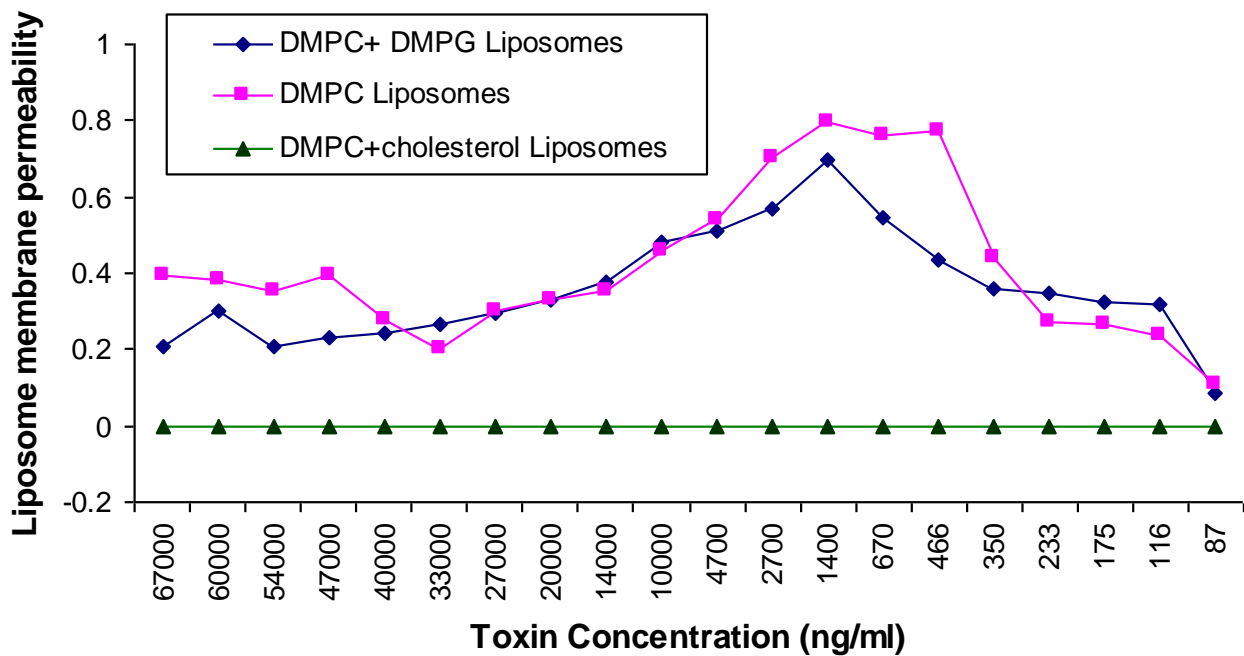
Figure 16 The degree of liposome membrane permeabilization of DMPC, DMPC+DMPG and DMPC+cholesterol liposomes after incubation with different concentrations of activated Cyt2Aa1 toxin.

4   Discussion

The δ-endotoxin Cyt2Aa1, found in parasporal inclusions of *Bacillus thuringiensis* subspecies *kyushuensis,* may be used as a lethal biological agent to the larvae of *Dipteran* insects in combination with other δ-endotoxins **[v]**. Because it is not easy to separate the δ-endotoxin Cyt2Aa1 from the naturally occurring parasporal inclusions for the purpose of conducting research and for its insecticidal activities, many attempts have previously been made to clone the δ-endotoxin Cyt2Aa1 *in vitro.* C. Gurkan and D.J. Ellar **[xxxv]** used an expression system *Pichia pastoris* yeast, but the system was not successful. B, Promdonkoy et al. constructed pGEM-Teasy-Cyt2Aa2 by cloning the Cyt2Aa2 gene into the pGEM-Teasy vector under control of the *lacZ* promoter and Cyt2Aa2 toxin was expressed successfully   **[xxxvii]**. Ellar et al. constructed the plasmid pUC18-Cyt2Aa1 by cloning the full-length Cyt2Aa1 gene into plasmid pUC18 vector between the *Sac*I and *Sph*I site and successfully expressed Cyt2Aa1 toxin **[xxxviii]**. In this work, we constructed the plasmid Cyt2Aa1-pET-30a (+) by cloning the full-length Cyt2Aa1 gene into plasmid pET-30a (+) vector. The cloned Cyt2Aa1- pET-30a(+)gene was found highly expressed and formed inclusions inside the *E. coli* BL21(DE3) cells. (see **Figure 12**). The cloning system that we developed has the advantage of very high yield of Cyt2Aa1 from dissolved inclusions (0.4 g of protoxin per liter of bacterial culture). This increase in yield over previous expression plasmids is likely due to the *E.coli*-specific codon optimization that was applied in the gene synthesis. Because of its high level of expression, the toxin is fairly pure

already directly after solubilization. Additional purification could be achieved by metal-chelating chromatography or gel filtration, at a pH of 10.5 or higher to maintain solubility.

The V186C and L189C mutants have been constructed for the purpose of cysteine labelling. The locations were chosen in the middle of β6 sheet (see **Figure 100**) which is likely to insert into the membrane **[xiv].** V186C was chosen because the position of valine at position 186 and leucine at 189 in the crystal structure is exposed to the outer surface which is an excellent position for labelling and to conduct fluorescence experiments. Moreover, the alignment with other members in the same family shows the presence of cysteine in the same position (see **Table 7**) in 4 members of the family (**Cyt1Aa1, Cyt1Aa3, Cyt1Ab1 and Cyt1Ba1).** So, we assumed that the replacing valine with cysteine at position 186 in β6 sheet in Cyt2Aa1 toxin should not affect the activity of the toxin. Remarkably, the activity of V186C is even higher than that of the wild type which makes it a good mutant for labelling without losing much activity. Further experiments will be done to test the activity on insect cells to determine whether or not the activity is also higher on those.

It was found that the Cyt2Aa1 toxin is completely inactive with DMPC+cholesterol liposomes, which indicates that cholesterol inhibits the liposome permeabilization with Cyt2Aa1 toxin. This was a surprising finding because both the normal target membranes in insect gut and sheep red cells, which were used in the activity assays, contain cholesterol. It is noteworthy that the concentration of toxin required to lyse red cell membranes is many times greater than that required for liposomes composed of DMPC only (compare **Figures 15** and **17**). The lower susceptibility of the cellular membranes may be due to their content of cholesterol.

46

Table 7 Amino acid sequence alignment of *β*6 sheet in Cyt2Aa1 toxin

Type	Amino acid sequence
Cyt1Aa1	V M Y *C* V P V G F E I K V
Cyt1Aa3	V M Y *C* V P V G F E I K V
Cyt1Ab1	V M Y *C* V P V G F E I K V
Cyt1Ba1	V M Y *C* V P I G F E I K V
Cyt2Aa1	V M A *V* L P *L* A F E V S V

The activity of activated Cyt2Aa1 toxin and mutants was obviously decreased with high concentration of toxin (see **Figure 14**). That phenomenon was observed both with red cells and with liposomes, so it's likely not due primarily to the membrane properties. The reason for this phenomenon maybe related to the pro-zone effect observed by Jursch**,** et,al **[xxxix]** with staphylococcal -α-toxin molecules during haemolytic activity testing. This phenomenon could be explained by a two-phase mechanism of oligomerization. Firstly, two or more monomers form a nucleus that is a small, partial oligomer. This reaction will be a higher order reaction that depends on the monomer concentration:

$$d[nucleus]/dt = k_{nucl}[monomer]^n$$

The nucleus then reacts with more monomers, until the oligomer is complete:

$$d[oligo_{n+1}]/dt = k_{growth}[nucleus][monomer]$$

$$d[oligo_{n+2}]/dt = k_{growth}[oligo_{n+1}][monomer]$$

Since the nucleation reaction is of higher order with respect to the monomer, it will be accelerated more strongly at high monomer concentration than the subsequent growth reaction. If the monomer concentration is high enough, what may happen is that rapid nucleation quickly forms many incomplete oligomers, most of which will then run out of available monomers before they can actually complete. So, the experimentally observed pro-zone effect for high Cyt2Aa1 toxin concentration could be supporting the proposed hypothesis of oligomeric pore forming mechanism of action.

The permeability of DMPC+DMPG liposomes was slightly lower than that of DMPC liposomes, indicating that DMPG, which is an anionic lipid with relatively smaller headgroup than DMPC, does not promote permeabilization.

It should be noted that the mechanism of action for Cyt2Aa1 toxin is still a matter of contention. While the membrane-damaging effect as such is not in dispute, there is disagreement whether permeabilization occurs through discrete pores of uniform size or rather involves a general destabilization of the bilayer, in a manner similar to that of detergents or antimicrobial peptides.

Discrete pores with a diameter of 1-2 nm have been characterized by Ellar et al. by using various osmotic protectants that has known viscometric radii **[xl].**These pores were assumed to be oligomeric, consisting of an estimated six monomers **[xiv].** Knowles et al. **[xli]** have shown the formation of potassium channels after incubation of the activated toxin with planar lipid bilayers. These authors also observed that upon incubation with liposomes with entrapped glucose, the

toxin caused glucose release. They raised the question if glucose passed through cation-selective channels or the toxin forms different kinds of openings in membranes. Recently, Ellar, et al. [**xxxviii**] confirmed the insertion of acrylodan-labelled Cyt2Aa1 toxin by recording a green-blue shift after incubation of the labelled toxin with RBC ghost membranes.

Butko et al. [**xlii**] have previously performed calcein release assays with Cyt1A with large unilamellar PC liposomes. As in our studies, calcein was released at low toxin concentration; however, they did not observe a decrease in calcein release at high concentration. Butko et al. calculated the number of toxin molecules required for the permeabilization of one liposome to 140. From this, they concluded the formation of discrete pores to be unlikely, since in that case a single oligomer, and accordingly a much smaller number of subunits, should suffice to permeabilize a liposome. They therefore favoured a detergent-like mechanism of action. Manceva, et al. [**xxxi**] used fluorescence photobleaching recovery to measure the diffusion coefficient of fluorescently labelled Cyt1A and epifluorescence microscopy to monitor the size of liposomes after incubation with Cyt1A. They found that upon addition of Cyt1A, liposomes were broken into smaller, faster diffusing objects. They presented this as evidence of a detergent-like mode of action of Cyt1A, because no change in size or morphology of the liposomes is expected when discrete pores are formed. That explanation would have more weight if the experiment had been done with biological membrane and over a wide range of toxin concentration.

All previous work did not show clear evidence of oligomeric pores. In our research, the pro-zone effect showed by high concentrations of the toxin could support the possibility of pore

formation based on the low activity that explained by formation of incomplete oligomers, which could not insert in membrane or form the desired pores. A molecular mass of 400 kDa had been separated by density gradient centrifugation from Triton X-100 extracted fraction of insect cell membrane treated with the toxin by E, Chow et al. [**xliii**]. This contradicts the assumption that only six monomers form the oligomer – 400 kDa is more like 16 subunits. That mass was assumed to be an oligomeric mass with out confirming the number of monomers contribution or assume that this mass could be aggregates of lipid-protein complex rather than an oligomeric mass. Moreover, when the same insect membrane treated with low concentration, the extracted fraction showed monomers rather than oligomer density. Moreover, the evidence in favour of pores has been reached on red cell membranes, whereas the evidence in favour of a detergent-like mode of action has been reached with liposomes. So, the mode of action might be different on both membranes. Furthermore, it had been reported the resistance of cell membranes to different detergents due to high cholesterol content of the extracted non-dissolved lipid bilayer [**xliv**]. In our experiments, the activity of Cyt2Aa1 toxin was inhibited with cholesterol liposomes, which may support the detergent-like mode of action.

When considering our own findings, the oligomeric pore formation appears to be supported by the pro-zone effect shown with higher concentrations of the toxin, while the detergent-like mode of action could be supported by the cholesterol inhibition of activity with artificial unilamellar liposomes. A final conclusion about the mechanism of action cannot be reached at this point.
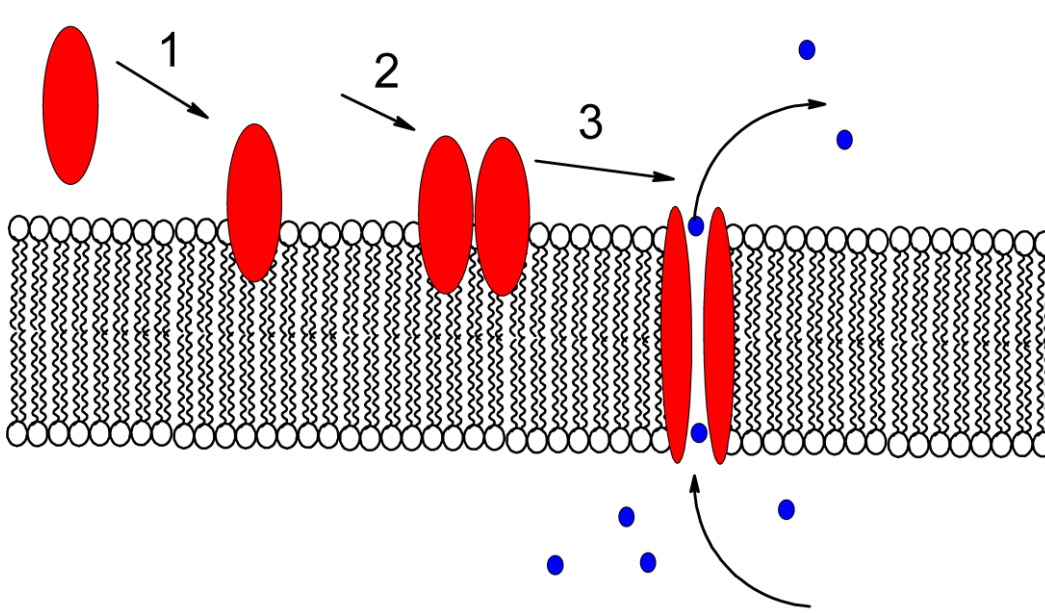
Figure 17: Pore forming model, 1: the activated soluble toxin accumulates in the extracellular phase. 2: toxin change confirmation to binds to lipids and inserts into the lipid bilayer 3: Oligomerization occurs and toxin form oligomeric pore then leakage of the intracellular fluid occurs through the formed pores.
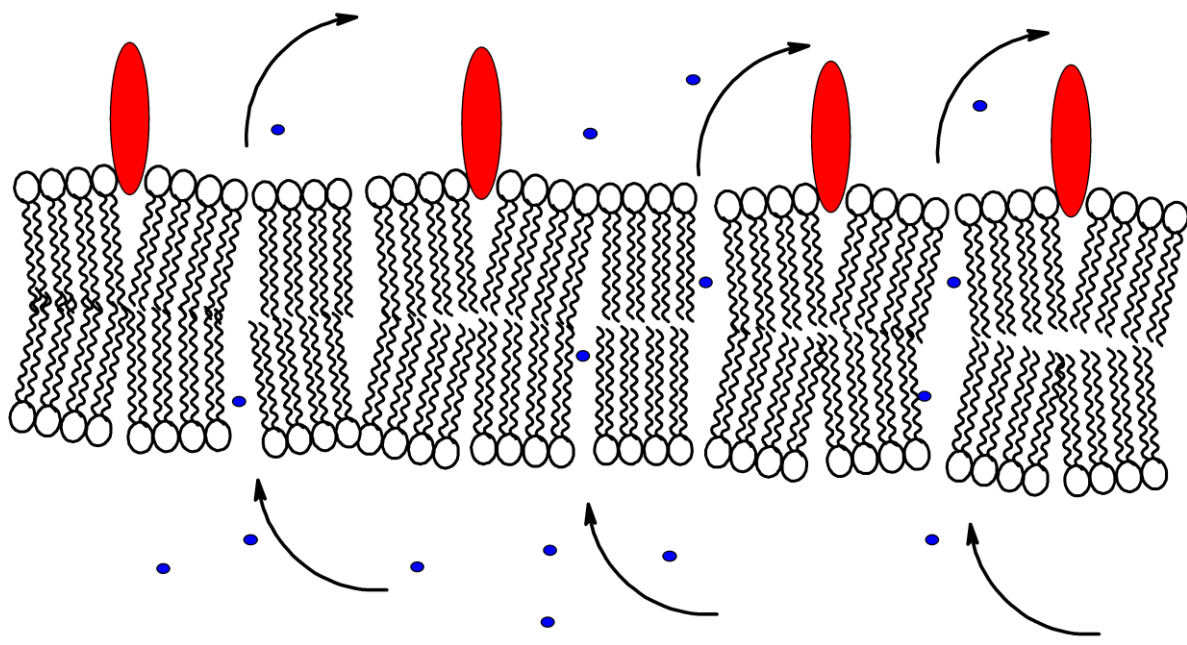
Figure 18 The detergent model, 1: the activated soluble toxin accumulates in the extracellular phase. 2: toxin change confirmation and binds to lipids. 3: The molecules insert only shallowly into the head group layer of the lipid bilayer. The distension of the head group layer disrupts the regular packing of the lipid molecules in the bilayer, causing membrane destabilization and membrane could be breaks up into protein/lipid complexes.

In the pore forming model, the leakage of the intracellular fluid occurs from the pores, but the membrane is still there even leaky (see **Figure 177**). In the detergent model, the toxin monomers could be adsorbed to the membrane surface and then haphazardly aggregate into large carpet-like structures. The molecules insert only shallowly into the head group layer of the lipid bilayer. The distension of the head group layer disrupts the regular packing of the lipid molecules in the bilayer, causing membrane destabilization and membrane could be broken up into protein/lipid complexes. This results in the leaking of cytoplasm and finally cell disintegration of the membrane.

Finally, another possible that Cyt2Aa1 toxin could work by both mechanisms could be considered because both evidences that supported both mechanisms had been obtained with high and low concentration of the toxin. So, the concentration could be the determining key to switch between both mechanisms. Another possible explanation is that both mechanisms could work with different time scale so that pores could be first formed and then disintegration of membrane by the toxin detergent-like action.

5 Conclusion

The expression of Cyt2Aa1 was successfully done with the new *E.coli* expression system. The yield of Cyt2Aa1 inclusions was more than expected when compared with other expression systems, which could be good for large scale industrial production. The newly constructed V186C mutant showed higher activity than the wild type, which could be beneficial if used in industrial production of most potent biological insecticide.The mechanism of action for Cyt2Aa1 toxin remains controversial and warrants more experiments to be done in future.

6 Future work

The long-term goals of our project also include the investigation of conformational changes using FRET (Fluorescence resonance energy transfer) studies. One probe will be placed on a cysteine residue and another one on a selenomethionine residue. This will allow the determination of the distance between the two labelled amino acids. If each residue labelled alone, this in turn will illustrate of the distance is fixed between pore forming monomers or distance is variable due to random aggregation. By repeating the experiment with different mutants, we hope to combine all data to derive a model for the toxin mode of action. For accuracy, all FRET experiments will be done with both physiological and artificial membranes.

Bibliography

[i] A.D, Barrett and S, Higgs. **Yellow fever: a disease that has yet to be conquered.** (2007) *Entomol,* **52**: 209–29.

[ii] E.D, Richter., P, Chuwers., Y, Levy., M, Gordon ., F, Grauer and J, Marzouk . **Health effects from exposure to organophosphate pesticides in workers and residents in Israel.** (1992) *Isr J Med Sci*, **28:**584-597.

[iii] V. Frankenhuyzen., K, Entwistle., J.S, Cory., M. J, Bailey and S, Higgs. **Bacillus thuringiensis, an environmental biopesticide: theory and practice.** (1993) *John Wiley & Sons*, Inc, 1–35.

[iv] J, Li ., P. A, Koni and D. J. Ellar . **Crystallization of a membrane pore-forming protein with mosquitocidal activity from *Bacillus thuringiensis* subspecies *kyushuensis.*** (2004) **23**: 290 – 293**.**

[v] M. W Parker and S.C. Feil, **Pore-forming protein toxins: from structure to function**. (2005) *Progr. Biophys. Mol. Biol,* **88:** 91–142.

[vi] M. R, Gonzalez., M, Bischofberger., L, Pernot., F. G. van der Goot and B. Freche. **Bacterial pore-forming toxins: The (w)hole story?** (2008) *Cell. Mol. Life Sci,* **65:** 493 – 507.

[vii] M.W, Parker. **Cryptic clues as to how water-soluble protein toxins form pores in membranes**. (2003) *Toxicon ,* **42:** 1-6.

[viii] Wiener; D, Freymann; P, Ghosh and R.M, Stroud. **Crystal structure of colicin Ia**. (1997) *Nature,* **385:** 461-464.

[ix] S.K, Buchanan., P, Lukacik., S, Grizot., R, Ghirlando ., M.M, Ali., T..J, Barnard., K.S, Jakes., P.K, Kienker and L, Esser . **Structure of colicin I receptor bound to the R-domain of colicin Ia: implications for protein import.** (2007) *Embo J,* **26:** 2594-260.

[x] J. E, Wedekind., C.B, Trame., M, Dorywalska., P, Koehl., T.M, Raschke., M, McKee., D, FitzGerald., R.J, Collier and D.B, McKay. **Refined Crystallographic Structure of Pseudomonas aeruginosa Exotoxin A and its Implications for the Molecular Mechanism of Toxicity**. (2001) *J.Mol.Biol,* **314:** 823-837.

[xi] N, Galitsky., V, Cody., A, Wojtczak ., D, Ghosh., J.R, Luft., W. Pangborn, L. English. **Structure of the insecticidal bacterial delta-endotoxin Cry3Bb1 of Bacillus thuringiensis.** (2001) *Acta Crystallogr,* Sect.D, **57:** 1101-1109.

[xii] L, Song., M.R, Hobaugh., C, Shustak., S, Cheley., H, Bayley and J.E, Gouaux. **Structure of staphylococcal alpha-hemolysin, a heptameric transmembrane pore**. (1996) *Science,* **274:** 1859-1866.

[xiii] S.J, Tilley., E.V, Orlova., R.J.C, Gilbert., P.W, Andrew and H.R, Saibil. .**Structural Basis of Pore Formation by the Bacterial Toxin Pneumolysin.** (2005) *Cell(Cambridge,Mass)* **121:** 247.

[xiv] J, Li., P.A, Koni and D.J, Ellar. **Structure of the mosquitocidal endotoxin cytB from Bacillus thuringiensis sp. Kyushuensis and implications for membrane pore formation**. (1996) *J. Mol. Biol.* **257:** 129–152.

[xv] C.H, Zhong., D. J, Ellar., A, Bishop., C, Johnson., S. S, Lin and E. R, Hart.**Characterization of a *Bacillus thuringiensis* delta-endotoxin which is toxic to insects in three orders.** (2000) *J. Invertebr. Patho,* **76**: 131–139.

[xvi] W, Thomas and D.J, Ellar. *Bacillus thuringiensis* **var israelensis delta-endotoxin: effects on cultured insect cells and mammalian cells.** (1982) *Proc. Int. Colloq. Invertebrate Pathology*, **3:** 59.

[xvii] N, Crickmore ., D.R, Zeigler., J, Feitelson., E, Schnepf., J, van Rie., D, Lereclus., J Baum., D.H, Dean. **Revision of the nomenclature for the *Bacillus thuringiensis* pesticidal crystal proteins.** (1998) *Microbiol. Mol. Biol. Rev*. **62**, 807–813.

[xviii] J, Li., J, Carroll ., and D.J, Ellar. **Crystal structure of insecticidal delta-endotoxin from *Bacillus thuringiensis* at 2.5Å resolution Nature**. (1991) *Nature,* **353**, 815-821.

[xix] R.J, Morse., T, Yamamoto and R.M, Stroud. **Structure of Cry2Aa suggests an unexpected receptor binding epitope**. (2001) *Structure,* **9:** 409-417.

[xx] P, Grochulski., L, Masson., S, Borisova., M, Pusztai-Care., J.L, Schwartz., R, Brousseau and   M, Cygler. **Bacillus thuringiensis CryIA(a) insecticidal toxin: crystal structure and channel formation.** (1995) *J.Mol.Biol,* **254:** 447-464.

[xxi] P, Boonserm., P, Davis., D.J, Ellar and J, Li . **Crystal Structure of the Mosquito-Larvicidal Toxin Cry4Ba and its Biological Implications** (2005) *J.Mol.Biol,* **348:** 363.

[xxii] S.C, Lin., Y.C, Lo., J.Y, Lin and Y.C, Liaw. **Crystal structures and electron micrographs of fungal valvotoxin A.** (2004) *J. Mol. Biol,* **343:** 477–491.

[xxiii] J, Li., D. J, Derbyshire., B, Promdonkoy and D. J, Ellar. **Structural implication for the transformation of the *Bacillus thurengiensis* δ-endotoxins from water-soluble to membran-inserted forms**. (2001) *Biochemical society*, **29:**571-577.

[xxiv] P.A, Koni and D.J, Ellar. **Biochemical characterisation of Bacillus thuringiensis cytolytic *δ* endotoxins.** (1994) *Microbiology* **140** : 1869–1880.

[xxv] P.A, Koni and D.J, Ellar. **Cloning and characterization of a novel *Bacillus thuringiensis* cytolytic δ-endotoxins**. (1993) *J. Mol. Biol.* **229:** 319-327.

[xxvi] A. Hilbeck and J.E.U. Schmidt. **Another View on Bt Proteins – How Specific are They and What Else Might They Do?**. (2006) *Biopestic. Int*, **2 (1):** 1-50.

[xxvii] H.P, Bietlot., I, Vishnubhatla., P.R, Carey., M, Pozsgay and H, Kaplan. **Characterization of the cysteine residues and disulphide linkages in the protein crystal of Bacillus thuringiensis.** (1990) *Biochem. J.* **267:**309–315.

[xxviii] S.S, Gill ., E.A, Cowles and P.V, Pietrantonio. **The mode of action of Bacillus thuringiensis endotoxins.** (1992) Annu Rev *Entomol*, **37:**615–63.

[xxix] R.A, de Maagd ., A, Bravo., C, Berry., N, Crickmore and H.E, Schnepf. **Structure, diversity and evolution of protein toxins from spore-forming entomopathogenic bacteria**. (2003) *Ann. Rev. Genet,* **37:** 409–433.

[xxx] T, Ganz. **mode of action of defensins and other antimicrobial peptides.** (2003) *nature,Immunolgy.* **3:** 710-720.

[xxxi] S. D, Manceva., M, Pusztai-Carey, P. S, Russo and P. Butko. **A detergent-like mechanism of action of the cytolytic toxin Cyt1A from** *Bacillus thuringiensis* **var.** *israelensis***.** (2005) Biochemistry **44:**589-597.

[xxxii] B, Promdonkoy and D. J, Ellar. **Structure-function relationships of a membrane pore-forming toxin revealed by reversion mutagenesis**. (2005) *Molecular Membrane Biology*, **22(4):** 227-337.

[xxxiii] B, Promdonkoy and D.J Ellar. **Membrane pore architecture of a cytolytic toxin from** *Bacillus thuringiensis***.** (2000) *Biochem* J**. 350:** 275-282.

[xxxiv] W.L. DeLano, **The PyMOL Molecular Graphics System**, DeLano Scientific, Palo Alto, CA, USA (2002).

[xxxv] C, Gurkan and D. J, Ellar**. Expression of the *Bacillus thuringiensis* Cyt2Aa1 toxin in *Pichia pastoris* using a synthetic gene construct.** (2003) *Biotechnol. Appl. Biochem*, **38**:25–33.

[xxxvi] F. M, Ausubel., R, Brent., R. E, Kington., J. G, Seidman., J. A, Smith and K. Struhl. **Short protocols in molecuar biology**, fourth edition. *WILEY* (1999).

[xxxvii] B, Promdonkoy., N, Chewawiwat., S, Tanapongpipat., P, Luxananil and S, Panyim. **Cloning and Characterization of a Cytolytic and Mosquito Larvicidal δ-endotoxin from *Bacillus thuringiensis* subsp. *Darmstadiensis*.** (2003) *Current microbiology,* **46:** 94–98.

[xxxviii] B, Promdonkoy and D. J, Ellar**. Investigation of the pore-forming mechanism of a cytolytic *δ*-endotoxin from Bacillus thuringiensis.** (2003) *Biochem. J.* **374**: 255–259.

[xxxix] R, Jursch., A, Hildebrand., G, Hobom., J, Tranum-Jensen., R, Ward., M, Kehoe and S, Bhakd. **Histidine Residues Near the N Terminus of Staphylococcal Alpha-Toxin as Reporters of Regions That Are Critical for Oligomerization and Pore Formation.** (1994) *Infection and immunology* , **64:** 2249-2256.

[xl] F. A, Drobniewski and D.J, Ellar. **Investigation of the membrane lesion induced in vitro by two mosquitocidal δ-endotoxins of Bacillus thuringiensis.** (1988) *Curr. Microbiol.* **16**:195–199.

[xli] B. H, Knowles., P. J, White., C. N, Nicholls and D. J, Ellar. **A broadspectrum cytolytic toxin from *Bacillus thuringiensis* var. *kyushuensis*.** (1992)*Proc. R. Soc. Lond. B Biol. Sci*. **248:**1–7.

[xlii] Butko, P., F. Huang., M. Pusztai-Carey and W. K, Surewicz. **Membrane permeabilization induced by cytolytic delta-endotoxin CytA from *Bacillus thuringiensis* var. *israelensis*.** (1996)*Biochemistry*, **35:**11355–11360.

[xliii] E, Chow., F. J. P, Singh and S.S, Gill. **Binding and aggregation of the 25 kilodalton toxin of Bacillus thuringiensis subsp. israelensis to insect cell membranes and alteration by monoclonal antibodies and amino acid modifiers.** (1989) *Appl. Environ. Microbiol.* **55 :** 2779–2788.

[xliv] N.M, Hooper. **Detergent-insoluble glycosphingolipid/cholesterol-rich membrane domains, lipid rafts and caveolae (Review).** (1999) *molecular membrane biology,* **16:** 145-156.